Brain, Behavior, & Immunity - Health 43 (2025) 100911

Contents lists available at ScienceDirect

Brain, Behavior, & Immunity - Health

journal homepage: www.editorialmanager.com/bbih/default.aspx

Biological sex, microglial signaling pathways, and radiation exposure shape cortical proteomic profiles and behavior in mice

Alexandra O. Strohm [a], Sadie Oldfield [d], Eric Hernady [c], Carl J. Johnston [b], Brian Marples [c], M. Kerry O'Banion [d,e], Ania K. Majewska [d,e,f,*]

[a] Departments of Environmental Medicine, University of Rochester Medical Center, Rochester, NY, 14642, USA
[b] Pediatrics, University of Rochester Medical Center, Rochester, NY, 14642, USA
[c] Radiation Oncology, University of Rochester Medical Center, Rochester, NY, 14642, USA
[d] Neuroscience, University of Rochester Medical Center, Rochester, NY, 14642, USA
[e] Del Monte Institute for Neuroscience, University of Rochester Medical Center, Rochester, NY, 14642, USA
[f] Center for Visual Science, University of Rochester Medical Center, Rochester, NY, 14642, USA

ARTICLE INFO

Keywords:
Microglia
Radiation
Sex
Behavior
Proteomics

ABSTRACT

Patients receiving cranial radiation therapy experience tissue damage and cognitive deficits that severely decrease their quality of life. Experiments in rodent models show that these adverse neurological effects are in part due to functional changes in microglia, the resident immune cells of the central nervous system. Increasing evidence suggests that experimental manipulation of microglial signaling can regulate radiation-induced changes in the brain and behavior. Furthermore, many studies show sex-dependent neurological effects of radiation exposure. Despite this, few studies have used both males and females to explore how sex and microglial function interact to influence radiation effects on the brain. Here, we used a system levels approach to examine how deficiencies in purinergic and fractalkine signaling, two important microglial signaling pathways, impact brain proteomic and behavioral profiles in irradiated and control male and female mice. We performed a comprehensive analysis of the cortical proteomes from irradiated and control C57BL/6J, P2Y12−/−, and CX3CR1−/− mice of both sexes using multiple bioinformatics methods. We identified distinct proteins and biological processes, as well as behavioral profiles, regulated by sex, genotype, radiation exposure, and their interactions. Disrupting microglial signaling, had the greatest impact on proteomic expression, with CX3CR1−/− mice showing the most distinct proteomic profile characterized by upregulation of CX3CL1. Surprisingly, radiation exposure caused relatively smaller proteomic changes in glial and synaptic proteins, including Rgs10, Crybb1, C1qa, and Hexb. While we observed some radiation effects on locomotor behavior, biological sex as well as loss of P2Y12 and CX3CR1 signaling had a stronger influence on locomotor outcomes in our model. Lastly, loss of P2Y12 and CX3CR1 strongly regulated exploratory behaviors. Overall, our findings provide novel insights into the molecular pathways and proteins that are linked to P2Y12 and CX3CR1 signaling, biological sex, radiation exposure, and their interactions.

1. Introduction

Cancers of the brain and central nervous system (CNS) stand as a formidable global health concern, with increasing incidence rates for both sexes worldwide (Ilic et al., 2023). Cranial irradiation is a common treatment for various malignancies, during which the normal tissue surrounding tumors is also irradiated. Consequently, radiation exposure is unfortunately often accompanied by normal tissue toxicities, resulting in long lasting effects on human health and cognition. Exposure to cranial irradiation can result in cognitive deficits, which are reported in up to 90% patients that survive 6 months post radiation treatment (Greene-Schloesser et al., 2012a, 2012b). Growing evidence suggests a critical role for microglia, the resident immune cells of the brain, in regulating cognitive function (Duggan et al., 2021). Microglia contribute to cognitive deficits following radiation, as evidenced by reduced radiation-associated neurological deficits in mice with depleted (Acharya et al., 2016; Krukowski et al., 2018a; Allen et al., 2020; Feng et al., 2016, 2018; Gibson et al., 2019) or inhibited (Jenrow et al., 2013;

* Corresponding author. Neuroscience, University of Rochester Medical Center, Rochester, NY, 14642, USA.
E-mail address: ania_majewska@urmc.rochester.edu (A.K. Majewska).

https://doi.org/10.1016/j.bbih.2024.100911
Received 22 November 2024; Accepted 23 November 2024
Available online 25 November 2024

Kalm et al., 2016; Markarian et al., 2021) microglia activity.

Microglia are crucial mediators of plasticity and engage in structural remodeling of synapses to impact cognition (Whitelaw et al., 2022; Cornell et al., 2022). One prominent pathway that governs microglia-neuron interactions (Badimon et al., 2020; Sipe et al., 2016; Cserep et al., 2020), dendritic spine loss (Sipe et al., 2016), and response to injury (Nimmerjahn et al., 2005; Davalos et al., 2005; Honda et al., 2001; Haynes et al., 2006) is purinergic signaling through the microglial receptor P2Y12. Activation of the P2Y12 receptor by ATP released during neuronal activity triggers microglial directed motility towards neurons and this allows microglia to inhibit overly active neurons during seizures (Badimon et al., 2020). Additionally, preventing P2Y12 activity inhibits microglia reactivity and has been therapeutically beneficial in several injury models (Gu et al., 2016; Webster et al., 2013; Yu et al., 2019). Furthermore, the loss of P2Y12 has behavioral effects in adult mice (Badimon et al., 2020; Lowery et al., 2021; Zheng et al., 2019; Peng et al., 2019; Uweru et al., 2024; Bollinger et al., 2023) and polymorphisms in P2Y12 have been linked to increased risk of epilepsy in humans (Wang et al., 2023). Nevertheless, the understanding of P2Y12 signaling in regulating brain homeostasis and its impact on cognitive impairment remains limited. As such, there is limited knowledge on how deficiencies in P2Y12 signaling may impact brain proteomic and behavioral profiles in a healthy setting as well as in the context of radiation exposure.

Another pathway that regulates neuronal health under physiological and pathological conditions is fractalkine (CX3CL1) signaling through the receptor CX3CR1 (Rogers et al., 2011; Corona et al., 2010; Hellwig et al., 2016; Sokolowski et al., 2014; Winter et al., 2020; Cardona et al., 2006; Gunner et al., 2019). CX3CL1 is released by neurons and binds to its G-protein coupled receptor, CX3CR1, which is specifically expressed on microglia and macrophages in the brain (Harrison et al., 1998). CX3CR1 deficient mice have defects in synaptic pruning (Gunner et al., 2019; Paolicelli et al., 2011; Arnoux et al., 2015; Nemes-Baran et al., 2020) and enhanced phagocytosis (Lowery et al., 2017; Milior et al., 2016) at different stages of development. These mice also display alterations in behaviors involved with learning and memory (Rogers et al., 2011; Winter et al., 2020), motor function (Rogers et al., 2011; Winter et al., 2020), and social engagement (Zhan et al., 2014). In humans, polymorphisms in CX3CR1 have been associated with coronary artery disease (Moatti et al., 2001), multiple sclerosis (MS) (Arli et al., 2013), amyotrophic lateral sclerosis (ALS) (Lopez-Lopez et al., 2014), and age-related macular degeneration (Tuo et al., 2004), as well as autism spectrum disorder (ASD) and schizophrenia (Ishizuka et al., 2017). Although there is substantial evidence highlighting the importance of both CX3CR1 and P2Y12 signaling in regulating brain health and function, how their loss affects molecular signatures, responses to radiation, and behavior have not been extensively characterized to date.

Understanding the role of microglia in modulating the effects of cranial irradiation on the brain and behavior could provide important insights into potential therapeutic interventions. As such, it is imperative to explore how different microglial signaling pathways and receptors regulate radiation responses in the brain. Additionally, sex differences are increasingly recognized in brain function and responses to radiation (Hinkle et al., 2019, 2023; Parihar et al., 2020), and in fact, interactions between sex and microglial function in radiation responses have been demonstrated (Hinkle et al., 2019), highlighting the need to include each of these factors in radiation exposure models. However, many studies examining radiation effects use either males or females of a single genotype, limiting our ability to understand how sex, microglial function, and radiation exposure can impact cognitive outcomes.

Here, we took a systems level approach and analyzed the cortical proteomes from male and female mice lacking receptors essential for canonical microglial signaling, P2Y12 and CX3CR1, that were exposed to a single dose of 10 Gy cranial irradiation and their respective controls. Using multiple bioinformatic methods, we identified proteins and distinct biological processes associated with sex, P2Y12 and CX3CR1 signaling, radiation exposure, and their interactions. Our results show that deficiencies in microglial signaling pathways had the greatest impact on the proteome, with Cx3CR1−/− mice exhibiting the most distinct proteome. We found expression levels of proteins impacted by radiation exposure in our mouse model correlated with RNA expression levels of normal-appearing non-tumor brain tissue from glioblastoma (GBM) patients treated with radiation therapy, suggesting some findings may have translational value. Moreover, we compiled a list of proteins whose expression changes in response to radiation were contingent on microglial signaling and/or sex, revealing varying sensitivity among biological processes and cell-types to radiation exposure. In conjunction, we assessed the behavior of these mice in the open field test and elevated plus maze. While we found evidence of interaction between sex, microglial function, and radiation for some locomotive behaviors, we did not observe interactions between these factors for exploratory behaviors. We found reduced exploratory behavioral outcomes in both CX3CR1−/− and P2Y12−/− mice compared to wild type mice, demonstrating that deficiencies in microglial signaling pathways can influence exploratory behavior. Altogether our results illuminate the complex relationships between microglial function and biological sex in regulating protein expression and animal behavior in the context of the physiological brain and in response to cranial irradiation.

2. Results

2.1. Loss of CX3CR1 had a distinct effect on the cortical proteome

We analyzed behavioral outcomes and cortical proteomic expression in adult male and female C57BL/6J, P2Y12−/− and CX3CR1−/− mice that were exposed to 10 Gy X-ray cranial irradiation (IR) or were unexposed (control). Mice were subjected to behavioral tests one month (days 38–43) following radiation exposure and cortices were harvested the week following behavior tests for mass spectrometry analysis to determine proteomic expression profiles (Fig. 1A). Our analysis included a total of 12 different experimental conditions (N = 7–11 mice per condition for behavior, N = 5 per condition for proteomics) and we identified a total of 6863 proteins across all our samples. We first sought to determine how loss of microglial signaling pathways (P2Y12−/− and Cx3CR1−/−; referred to as genotype), biological sex, radiation exposure, and their interactions contribute to variation in proteomic expression (Fig. 1). Genotype had the strongest impact on the proteome (mean F ratio from ANOVA = 10.89), followed by sex (mean F ratio from ANOVA = 3.00), and radiation exposure (mean F ratio from ANOVA = 2.98; Fig. 1B). Principal component analysis of proteomic samples revealed a clear separation of CX3CR1−/− mice from C57BL/6J and P2Y12−/− mice (Fig. 1C), suggesting that loss of CX3CR1 had the largest effect on the cortical proteome.

2.2. Co-expressed cortical proteins are influenced by sex, microglial signaling, and radiation exposure

Next, we used a systems level approach to identify specific proteomic signatures associated with differences in biological sex, microglial signaling, or radiation exposure by performing a weighted protein co-expression network analysis (WPCNA) on the cortical proteomes. In this approach, we identified groups of proteins (modules) that exhibit coordinated expression patterns across all samples, and then determined which of these modules were associated with different experimental traits. Our network consisted of 16 co-expression modules (Fig. 2A) which, using module eigenproteins (MEs), were found to be associated with sex (black and purple), radiation (midnight blue, yellow, magenta and blue), P2Y12−/− (magenta, red, green, tan, pink, salmon, turquoise, midnight blue, purple), and CX3CR1/- (greenyellow, brown, turquoise, midnight blue, purple, tan, black, yellow, red, green). It is interesting to note that a greater number of modules correlated with microglial signaling than with either sex or radiation, corroborating that

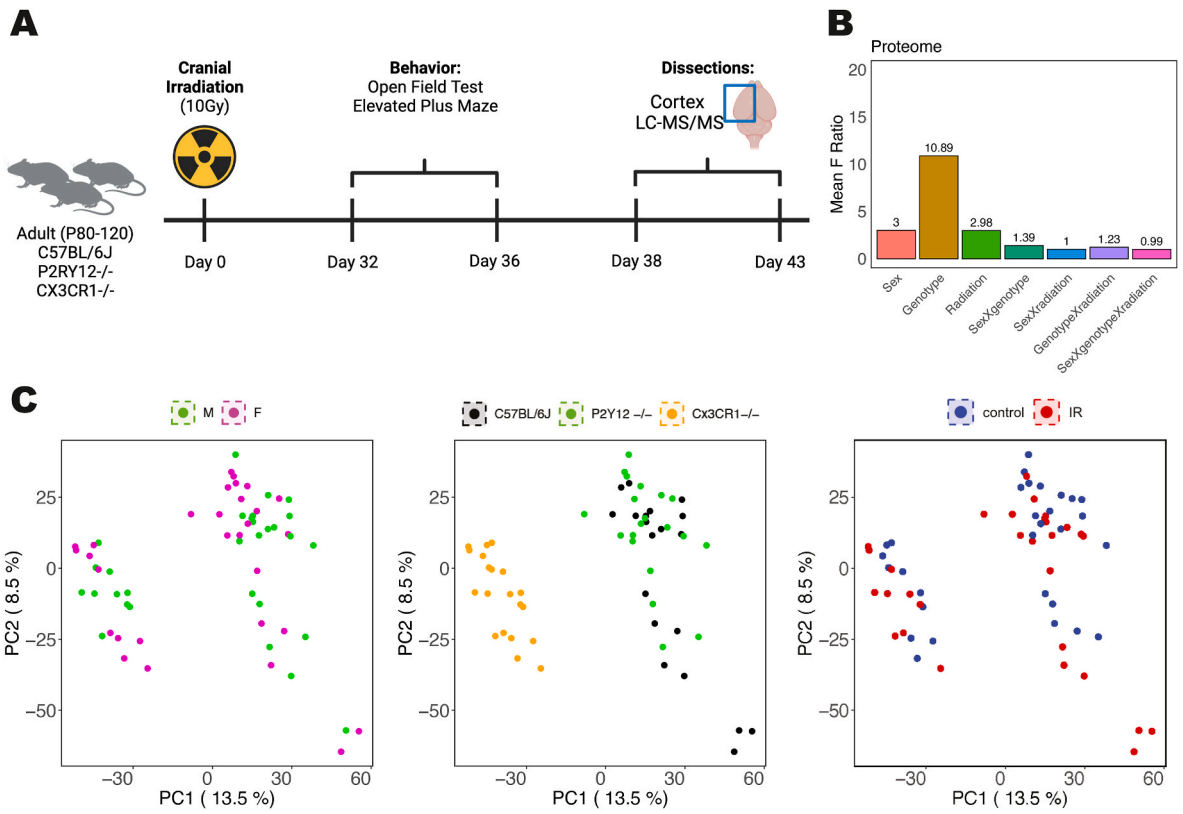

Fig. 1. Experimental design and characterization of the cortical proteome of IR and control C57BL/6J, P2Y12−/− and CX3CR1−/− mice of both sexes. A) Experimental design showing the timeline of cranial irradiation, behavioral assays, and cortical dissections. B) The effects of sex, genotype, radiation exposure, and their interactions on the proteome. C) Sample variation revealed by Principal Component (PC) analysis color-coded by sex, genotype, and radiation exposure. N = 5 mice per sex/group/genotype. The values for panel B) were determined by using a linear model followed by ANOVA. The F ratio in ANOVA represents the ratio of two mean square values. A larger F ratio indicates a higher variation among group means and generally corresponds with a lower p-value. Radiation exposure is abbreviated as IR. PC stands for "principal component."

microglial function (especially through CX3CR1 signaling) has the strongest impact on the proteome (Fig. 1B &C). Additionally, many modules were regulated by multiple traits, suggesting that these modules may reflect functional units that are co-regulated by different conditions. We further analyzed the relationship between MEs and traits to assess the relatedness of co-expression modules, finding strong correlations between the grey and greenyellow modules, the turquoise module and CX3CR1−/− genotype, as well as the red module and P2Y12−/− genotype (Pearson correlation coefficient >0.8, Fig. 2B).

2.3. *Biological processes linked to sex differences through Co-expressed and correlated proteins*

Next we performed gene ontology enrichment analysis to identify biological processes associated with proteins in modules which were influenced by sex, microglial signaling, and radiation (Fig. 3). To identify biological processes that differed by sex, we performed gene ontology enrichment analysis of proteins in the black module. We found proteins in the black module were associated with biological processes which regulate protein structural assembly and cellular responses to heat and stress (Fig. 3A). The black ME was significantly upregulated in males compared to females of all genotypes, further supporting its association with sex-differences (Fig. 3B). Hierarchical clustering of the top 20 intramodular hub proteins for the black module did not reveal a total separation by sex (Supplemental Fig. 1A), suggesting that other factors may regulate these proteins (Supplemental Fig. 5A). Further investigation using a linear model followed by ANOVA revealed a main effect of microglial signaling (genotype) and weak evidence of an interaction between microglial signaling and radiation for the black ME (Supplemental Fig. 5A), suggesting these factors may also regulate the expression of proteins in the black module.

To further identify proteins and biological processes associated with sex differences, we also performed gene ontology enrichment analysis of proteins whose expression patterns significantly correlated with biological sex. We found proteins whose expression patterns correlated with biological sex were also associated with biological processes that regulated protein assembly, in addition to cellular toxicological responses and several metabolic processes (Supplemental Fig. 6A). Expression across all samples of the top 20 proteins that correlated with biological sex included x-linked proteins Eif2s3x, Ddx3x, Pbdc1, which were unsurprisingly upregulated in females (Supplemental Fig. 1B). Additionally, these top 20 proteins included Hsp90aa1, Ddx3x, Eif2s3x, Prdx6, which were also upregulated in females aligning with the findings of others (Weis et al., 2021; Wingo et al., 2023; Weickert et al., 2009; Distler et al., 2020; Xu et al., 2006). Notably, both Selenow and Gpx1 have previously been identified to be upregulated in female compared to male microglia across several brain regions (Barko et al., 2022). When comparing top proteins identified through correlation analysis with those in the black module from the WPCNA analysis, we found several of these top 20 proteins overlapped with the top 20 intramodular hub proteins for the black module, including Ublcp1, Rbm3, Pdia4, Mthfd1l, Hsd11b1, HSP90a, and Cirbp (Supplemental Figs. 1A–B). This highlights a strong link between these proteins and sex.

2.4. *Co-expressed and correlated proteins linked to radiation exposure indicate altered immune, glia, and neuronal processes*

To identify biological processes influenced by radiation exposure, we

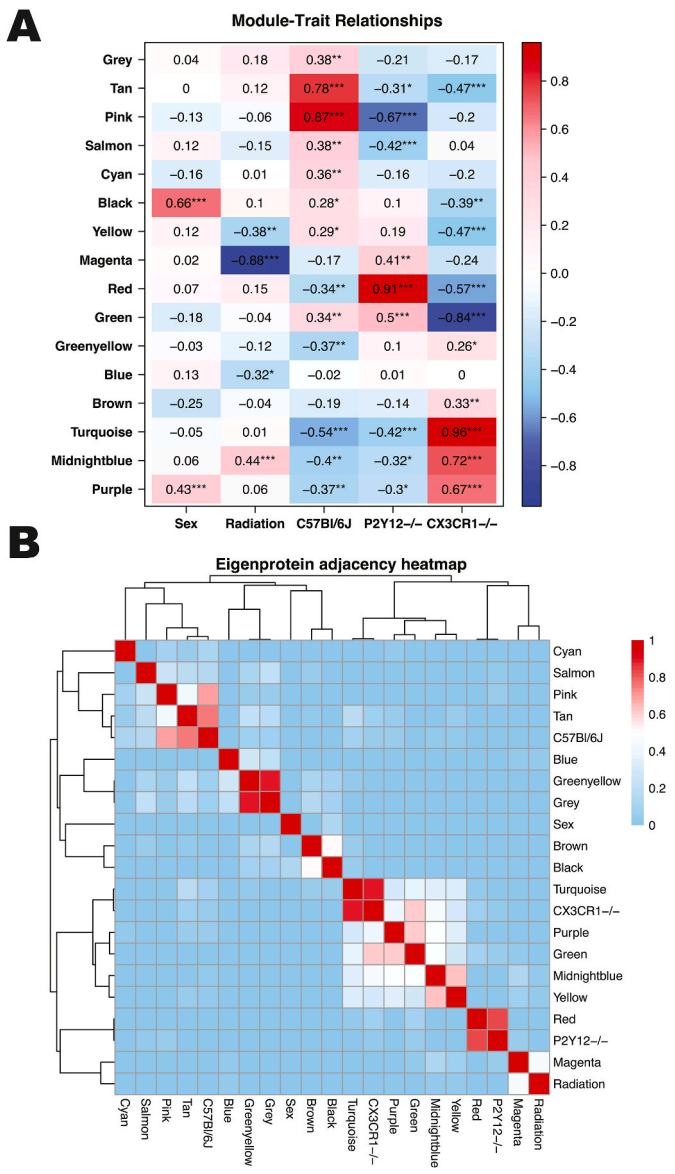

Fig. 2. Impact of sex, genotype, and radiation exposure on co-expression networks of the mouse cortical proteome. A) The correlation between module eigenproteins (MEs) and sex, radiation exposure, and C57BL/6J. The values in the heatmap are Pearson's correlation coefficients. Significant correlations are defined as *p < 0.05, **<0.01, ***<0.001. Modules with positive values (red) indicate a positive correlation, while modules with negative values (blue) indicate a negative correlation, of MEs with male sex, radiation, C57BL/6J, P2Y12−/− or CX3CR1−/− genotype. The Grey module represents proteins that were not assigned to other modules. B) Heatmap of eigenprotein adjacency matrix. Each row and column represent a module eigenprotein or trait. Red represents a positive correlation and blue represents a negative correlation. N = 5 mice per sex/group/genotype. Radiation exposure is abbreviated as IR.

performed gene ontology enrichment analysis of proteins in the magenta module, finding these proteins are involved in several immune related pathways as well as metabolic pathways and synapse pruning (Fig. 3C). The magenta ME was significantly downregulated in irradiated mice compared to control mice in all genotypes, further corroborating its relation to radiation exposure (Fig. 3D). Hierarchical clustering of the top 20 intramodular hub proteins in the magenta module showed a clear separation of P2Y12−/− mice from C57BL/6J and CX3CR1−/− mice, with a less clear separation based on radiation exposure (Supplemental Fig. 2A). Interestingly, the magenta module was also significantly positively correlated with the P2Y12−/− genotype, though the Pearson correlation coefficient was notably lower than that of radiation exposure (Fig. 2A). Further analysis using a linear model followed by ANOVA confirmed a significant main effect of genotype for the magenta ME (Supplemental Fig. 5A), strengthening the evidence that genotype regulates the proteins in this module. However, given the magenta ME was significantly downregulated in irradiated mice compared to control mice in all genotypes (Fig. 3D), this likely indicates that proteins in this module are strongly impacted by radiation exposure regardless of genotype.

We then identified proteins that were significantly correlated with radiation exposure and performed gene ontology enrichment analysis of these proteins, finding that this set of proteins was associated with the immune response as well as glial cell development (Supplemental Fig. 6B). Expression across all samples of the top 20 proteins that correlated with radiation exposure is shown in Supplemental Fig. 2B. We found several of these proteins overlapped with the top 20 intramodular hub proteins for the magenta module, including Rgs10, Crybb1, Vcan, Ephx1, C1qa, Scrg1, Hexb, Gnaz, and Bcas1 (Supplemental Fig. 2A and B). Consistent with previous results (Markarian et al., 2021; Osman et al., 2020), proteins in the complement pathway, including C1qa, C1qc, and C1qb, and microglial proteins Hexb, Rsg10, Crybb1 and Ctss, were decreased with radiation exposure. Additionally, Ephx1 and Ifit3 were upregulated, consistent with previous observations of their gene products increasing in hippocampal microglial following radiation exposure (Osman et al., 2020). Notably, Gfap, an intermediate filament protein specific to astrocytes, was upregulated (Supplemental Fig. 2B), reflecting the astrocyte activation and gliosis, which has been reported in the hippocampus following radiation exposure (Moravan et al., 2011). Altogether, these findings show changes in cortical proteomic expression indicative of an altered immune and glial response, as well as neuronal changes following radiation exposure.

2.5. Distinct biological processes are associated with proteins linked to genetic deficiencies in microglial signaling pathways

No studies to our knowledge have characterized the cortical proteomes of Cx3Cr1−/− and P2Y12 −/− mice. We therefore evaluated the proteomic profiles associated with the P2Y12−/− and CX3CR1−/− genotypes by performing gene ontology enrichment analysis of proteins in the red and turquoise modules. The red module proteins were associated with biological processes related to translation and several metabolic pathways involving Acetyl-CoA (Fig. 3E). Previous reports demonstrate antagonistic activity of Acetyl-CoA and its derivatives at P2Y12 receptors (Manolopoulos et al., 2008), supporting the link between Acetyl-CoA and P2Y12 signaling. The red module ME was upregulated in P2Y12−/− mice compared to C57BL/6J and CX3CR1−/− mice, confirming its association with the P2Y12−/− genotype (Fig. 3F). Hierarchical clustering of the expression across all samples of the top 20 intramodular hub proteins in the red module showed a clear distinction between P2Y12−/− and the other genotypes (Supplemental Fig. 3A). Although analysis using a linear model followed by ANOVA found a significant main effect of genotype and radiation, as well as a significant interaction between sex, genotype, and radiation exposure on the red ME (Supplemental Fig. 5A), post hoc analysis showed a significant upregulation of the red ME in P2Y12−/− mice relative to the other conditions, further confirming the association of the red module with the P2Y12−/− genotype.

We found proteins highly correlated with the P2Y12−/− genotype were also associated with several metabolic processes, as well as processes related to translation, including the formation of cytoplasmic translation initiation complex, which was associated with proteins in the red module (Fig. 3E & Supplemental Fig. 6C). This may indicate that P2Y12−/− impacts metabolism on a broader scale. Expression across all samples of the top 20 proteins that correlated with the P2Y12−/− genotype is shown in Supplemental Fig. 3B, with hierarchical clustering showing a clear distinction between P2Y12−/− and the other

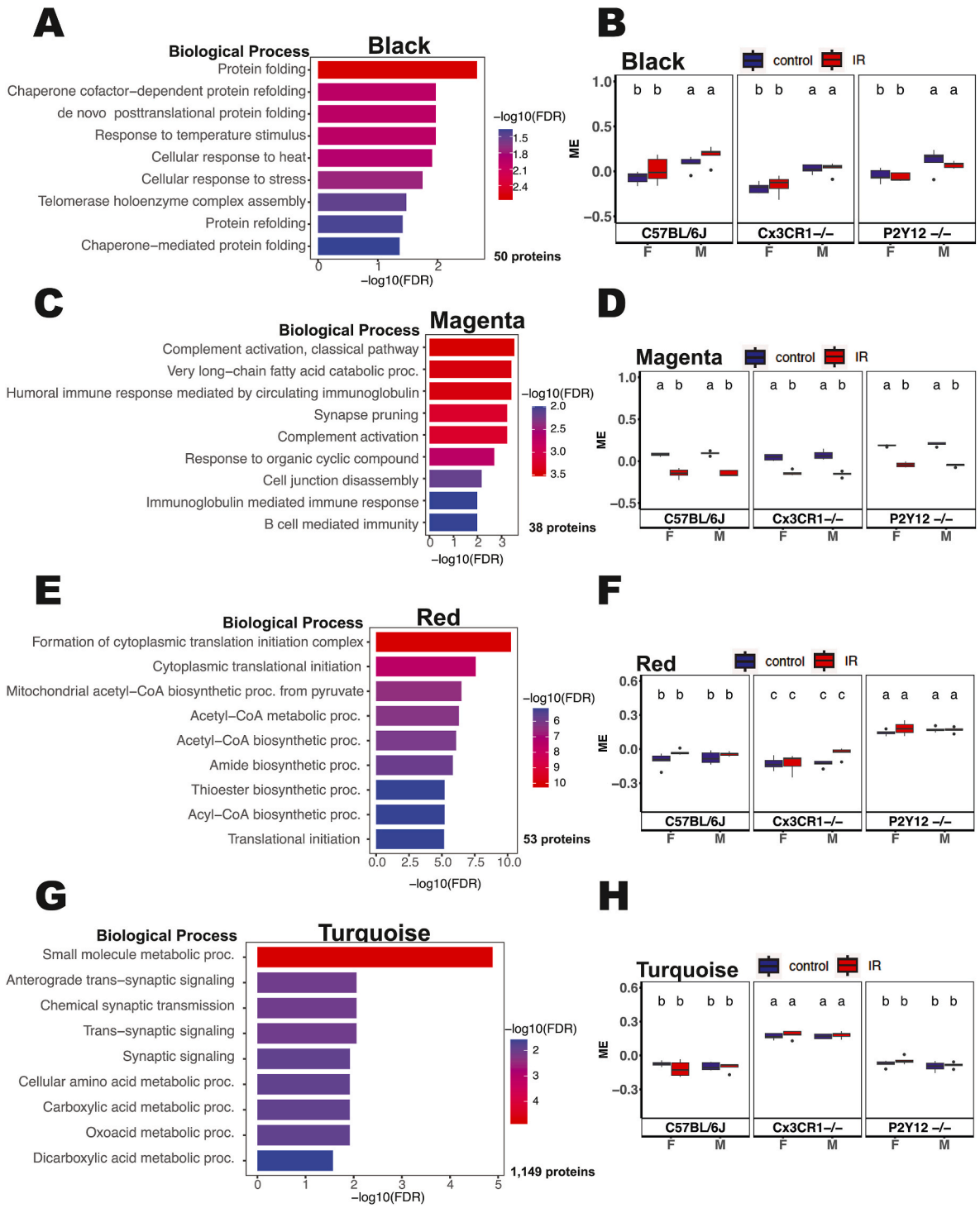

Fig. 3. Biological processes associated with cortical protein co-expression networks impacted by sex, genotype, and radiation exposure. The top ten gene ontology terms for biological processes associated with the 50 proteins in the Black module A), 38 proteins in the magenta module C) 53 proteins in the Red module E) and 1149 proteins in the turquoise module G). Module eigenproteins (MEs) in the Black B), Magenta D), Red F), and Turquoise H) modules across genotype (C57BL/6J, P2Y12−/− and CX3CR1−/−), sex (male and female), and radiation exposure (IR and control). The top and bottom lines in the box plots represent the upper and lower quartile values, and the center lines represents the median. ShinyGO verision 0.77 was used to create bar plots in A,C,E,G. Group means with the same letter are not significantly different, whereas group means with different letters are significantly different. Significance was determined by a linear model followed by ANOVA and Tukey's post hoc testing ($p < 0.05$). N = 5 mice per sex/group/genotype. Radiation exposure is abbreviated as IR. False Discovery Rate is abbreviated as FDR.

genotypes. We found overlap of many of the top 20 proteins that correlated with the P2Y12−/− genotype and the top 20 intramodular hub proteins for the red module, including P2Y12, Wdfy1, Dlat, Dld, Kcnb1, Tars3, Glud1, Acat1, Ogdh, Pdhx, Dnajc5, Slc25a24, Eif3c, and Kars1 (Supplemental Figs. 3A and B). This supports a robust association of these proteins with the P2Y12−/− genotype.

Proteins in the turquoise module were associated with numerous synaptic signaling and metabolic processes (Fig. 3G), supporting the

robust evidence that links CX3CR1 signaling to neuronal physiology (Rogers et al., 2011; Corona et al., 2010; Hellwig et al., 2016; Sokolowski et al., 2014; Winter et al., 2020; Cardona et al., 2006; Gunner et al., 2019). The turquoise ME was significantly upregulated in CX3CR1−/− mice compared to C57BL/6J and P2Y12−/− mice, confirming its association with the Cx3CR1−/− genotype (Fig. 3H). Further analysis using a linear model followed by ANOVA confirmed a significant main effect of genotype on the turquoise module, and weak evidence for an interaction between genotype and radiation exposure on the turquoise module (Supplemental Fig. 5A). This suggests radiation exposure may impact the expression of some proteins in the turquoise module. Hierarchical clustering of the top 20 intramodular hub proteins

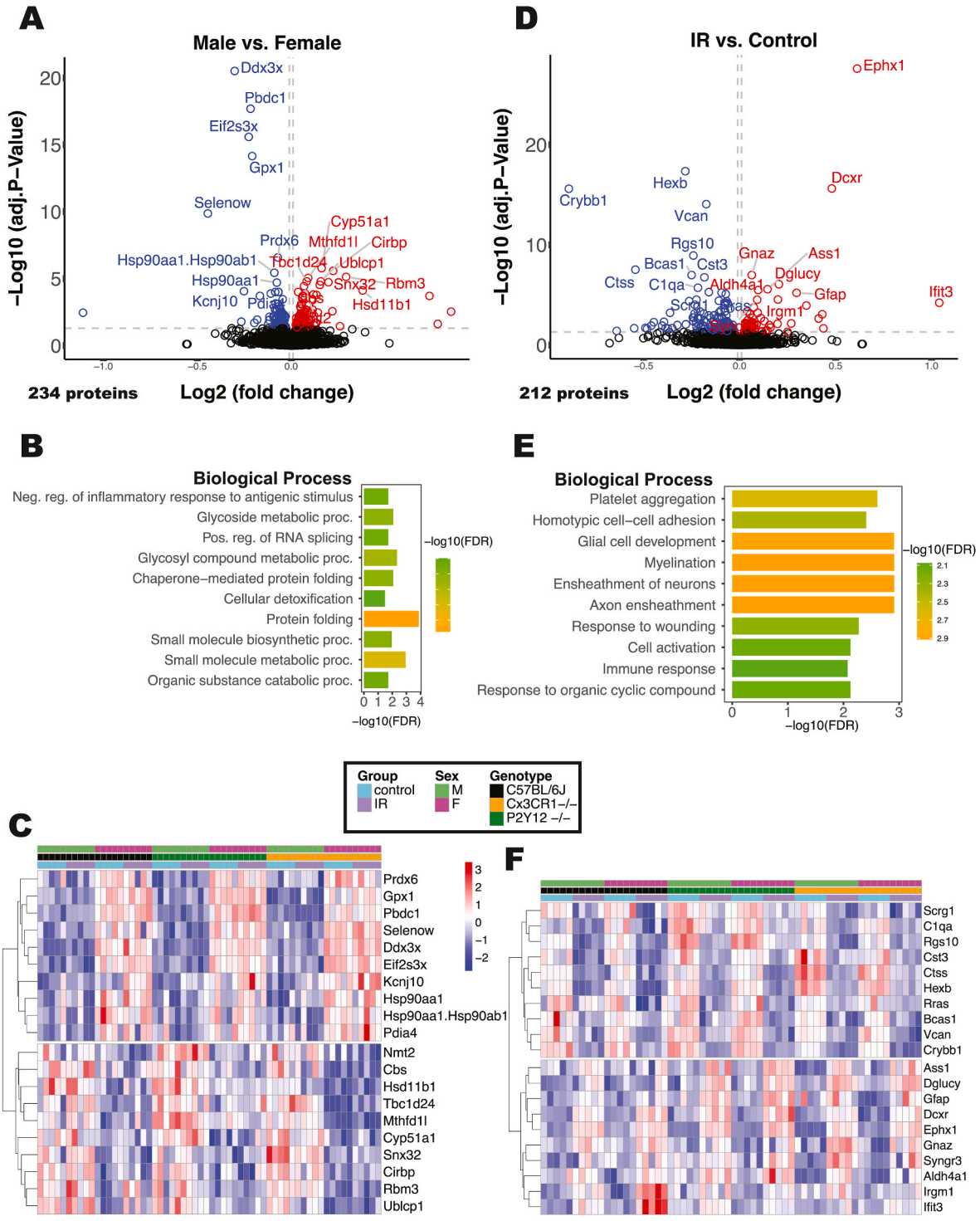

Fig. 4. Impact of sex and radiation exposure on differential protein expression and gene ontology enrichment analysis in the mouse cortical proteomes. Volcano plots showing differential protein expression (Student's t-test, Benjamin-Hochberg corrected $p < 0.05$) between male and female mice A) as well as irradiated and control mice D). The top 20 differentially expressed proteins (lowest p-value) are labeled. Red proteins are significantly upregulated and blue proteins are significantly downregulated. Gene ontology enrichment of biological processes associated with differentially expressed proteins between sex B) and radiation exposure E). Heatmaps showing the top 10 upregulated and top 10 downregulated proteins for sex C), radiation exposure F). ShinyGO verision 0.77 was used to create bar plots in B and E. N = 5 mice per sex/group/genotype. Radiation exposure is abbreviated as IR. False Discovery Rate is abbreviated as FDR.

in the turquoise module showed a clear distinction between CX3CR1−/− and the other genotypes (Supplemental Fig. 4A).

Proteins that were significantly correlated with the CX3CR1−/− genotype were associated with synaptic and metabolic processes, most of which overlapped with those identified to be associated with the turquoise module (Fig. 3G & Supplemental Fig. 6D). Hierarchical clustering of the top 20 proteins that correlated with the CX3CR1−/− genotype showed a clear distinction between CX3CR1−/− and the other genotypes (Supplemental Fig. 4A). Several of the top proteins that significantly correlated with the CX3CR1−/− genotype (Supplemental Fig. 4B) were also identified as intramodular hub proteins for the turquoise module (Supplemental Fig. 4A), including Rab2, Iars2, Cx3cl1, Nudt3, Uchl1, Rab2a, Hars1, Nipsnap1, Prps2, Plcb1, Ift22, Pck2, and Cnksr2. This highlights a strong connection between these proteins and the CX3CR1−/− genotype. Notably, CX3CL1, the ligand for CX3CR1, was increased in CX3CR1−/− mice relative to other genotypes, suggesting a compensatory regulatory mechanism for this molecule (Supplemental Figs. 4A and B). Overall, these results show distinct changes in biological processes and protein signatures associated with P2Y12−/− and CX3CR1−/− genotypes, highlighting different roles of these microglial signaling pathways in regulating brain homeostasis.

2.6. *Differential expression analysis reveals consistent proteins and biological processes linked to sex and radiation exposure*

While WPCNA analysis gave us a network view, identifying protein clusters that might serve as functional modules associated with sex, microglial function and radiation, we next performed differential expression and gene ontology enrichment analysis which allowed us to identify differentially expressed proteins (DEPs) across our samples (Fig. 5 and 6). We found 234 DEPs between males and females, with 126 upregulated proteins and 108 downregulated proteins (Fig. 4A). Gene ontology enrichment analysis of these DEPs revealed the same biological processes as our correlation analysis with respect to sex, with the addition of organic substance catabolic processes, furthering substantiating our previous results (Fig. 4B, Supplemental Fig. 6A). Indeed, the top 20 DEPs by sex were the same proteins found to be highly correlated with sex (Fig. 4C, Supplemental Fig. 1B). Fifty-seven of the 234 DEPs

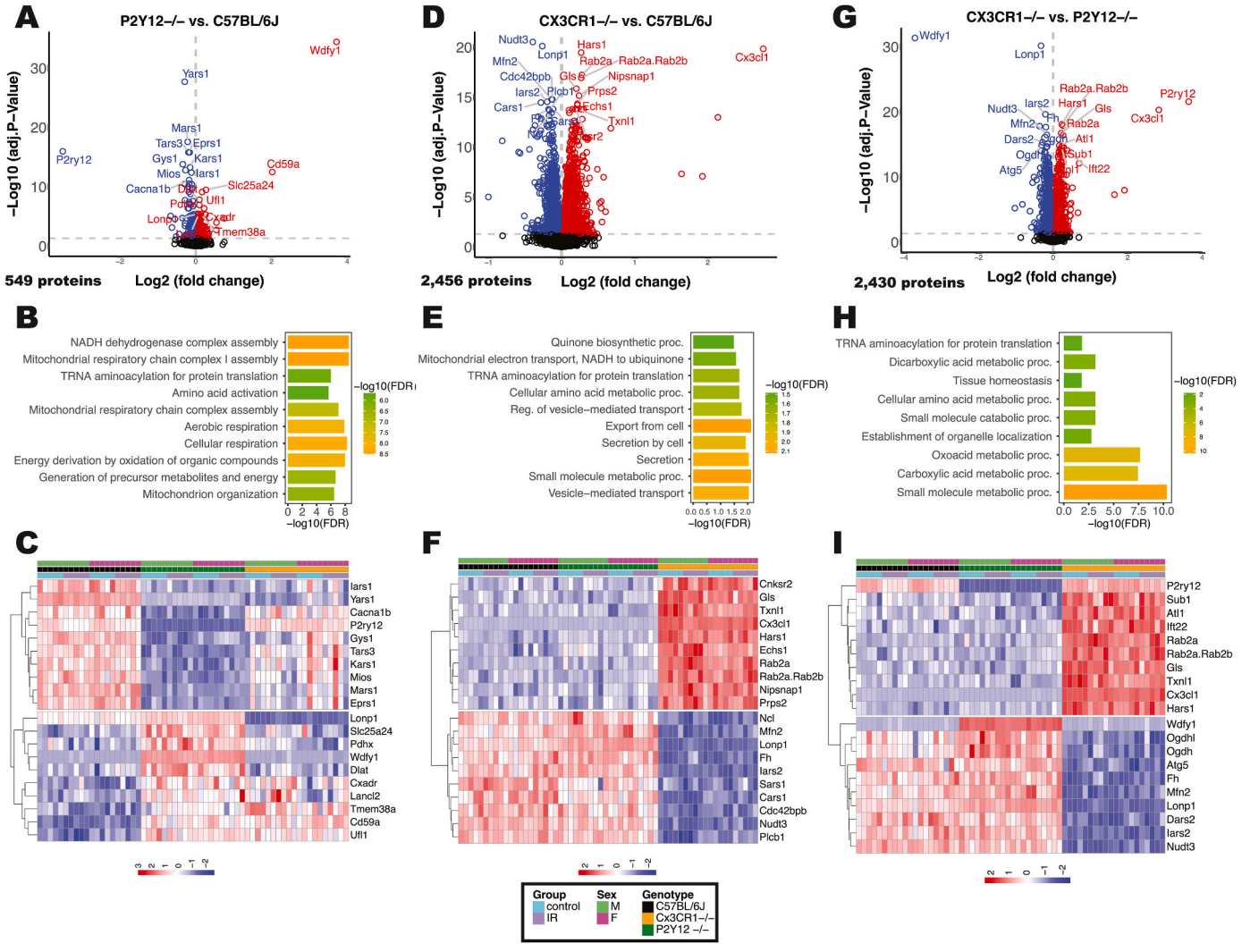

Fig. 5. Impact of deficiencies in microglial signaling pathways on differential protein expression and gene ontology enrichment analysis in the mouse cortical proteomes. Volcano plots showing differential protein expression (Student's t-test, Benjamin-Hochberg corrected $p < 0.05$) P2Y12−/− and C57BL/6J mice A), CX3CR1−/− and C57BL/6J mice D), and CX3CR1−/− and P2Y12−/− mice G). The 20 differentially expressed proteins (lowest p-value) are labeled. Red proteins are significantly upregulated and blue proteins are significantly downregulated. Gene ontology enrichment of biological processes associated with differentially expressed proteins between genotype comparisons (B,E,H). Heatmaps showing the top 10 upregulated and top 10 downregulated proteins for genotype comparisons (C,F,I). ShinyGO verision 0.77 was used to create bar plots in B,E,H. N = 5 mice per sex/group/genotype. Radiation exposure is abbreviated as IR. False Discovery Rate is abbreviated as FDR.

were recently also identified with sex-biased expression by Wingo et al. (2023) in human tissue (Supplemental Table 1).

We found 212 DEPs between irradiated and control mice, with 72 upregulated and 140 downregulated proteins (Fig. 4D). These proteins were linked to the same biological processes as our correlation analysis with respect to radiation exposure, including glial cell development, myelination, ensheathment of neurons, response to wound healing, cell activation, and the immune response (Fig. 4E, Supplemental Fig. 6B). All top 10 downregulated DEPs were the same proteins shown in Supplemental Fig. 2B to be highly correlated with radiation exposure (Scrg1, C1qa, Rgs10, Cst3, Ctss, Hexb, Rras, Bcas1, Vcan and Crybb1, Fig. 4F). Most of the top 10 upregulated DEPs were also identified in Supplemental Fig. 2B to be highly correlated with radiation exposure, with the addition of Syngr3 (Fig. 4F). Altogether, our identification of proteins and processes from differential expression analysis by sex and radiation exposure corroborate our findings from the WPCNA and correlation analysis with respect to these conditions.

Next, we sought to determine whether the radiation effects on protein expression in mouse cortical tissue may be evident in human patients treated with radiation therapy. We compared the change in expression levels of DEPs impacted by radiation exposure in our mouse model to the change in RNA expression levels of normal-appearing non-tumor brain tissue from glioblastoma (NAGBM) patients treated with radiation therapy. We found the $\log_2$fold-change in expression of DEPs between irradiation and control mice significantly correlated with the $\log_2$fold-change in gene expression of the irradiated treated glioblastoma human tissue and region-matched brain tissue from unaffected control individuals (Supplemental Fig. 7A). When limiting the comparison to the top DEPs impacted by radiation exposure in our experiment, we also observed a significant correlation with expression changes in NAGBM tissue (Supplemental Fig. 7B). However, the directionality of the $\log_2$fold-changes between humans and mice differed for some proteins, possibly due to differences in the time that tissue was harvested post-IR exposure or the inconsistency in comparing RNA to protein expression changes. Overall, these results suggest some of our findings in mice may have translational value.

2.7. *Differential expression analysis reveals unique proteomic signatures linked to deficiencies in microglial signaling*

When examining DEPs with respect to genotype, we found 549 DEPs in P2Y12−/− mice vs. C57BL/6J mice, with 270 upregulated and 279 downregulated DEPs (Fig. 5A). These proteins were associated with processes involved in energy metabolism, mitochondria function, and respiration (Fig. 5B). Notably, these processes were distinct from those identified through WPCNA and correlation analysis. However, some of the top 10 upregulated and downregulated DEPs overlapped with those identified to be highly correlated with the P2Y12−/− genotype, including P2Y12, Cacna1b, Tar3, Mios, and Kars1, indicating some consistency between bioinformatic methods (Fig. 5C, Supplemental Fig. 3B). Other DEPs included upregulated proteins Lonp1, Cxadr, Lancl2, Tmem38a, Cd59a, and Ufl1 and downregulated proteins Lars1, Yars1, Gys1, Mars1, and Eprs1 (Fig. 5C).

When comparing CX3CR1−/− mice to C57BL/6J mice, we found 2456 DEPs, with 1418 upregulated and 1038 downregulated DEPs (Fig. 5D). These were associated with metabolic biological processes, as well as those involving cellular transport and secretion (Fig. 5E). The top 10 upregulated DEPs included Cnkrs2, Gls, Txnl1, Cx3Cl1, Hars1, Rab2a, Nipsap1, and Prps2, which were also identified as highly correlated with the CX3CR1−/− genotype (Fig. 5F, Supplemental Fig. 4B), as well as Rab2a.Rab2b and Echs1. The top 10 downregulated DEPs included Mfn2, Lonp1, Fh, Lars, Nudt3, and Plcb1, which were also identified as highly correlated with the CX3CR1−/− genotype (Fig. 5F, Supplemental Fig. 4B), as well as Ncl, Sars1, Cars1, and Cdc42bpb.

We found 2430 DEPs in CX3CR1−/− mice vs. P2Y12−/− mice, with 1389 proteins upregulated and 1041 proteins downregulated (Fig. 5G). These DEPs were associated with several metabolic processes (Fig. 5H), and the top DEPs included Wdfy1, Lonp1, Cx3Cl1, and P2Y12 (Fig. 5I). Notably, CX3CR1−/− mice had the greatest number of DEPs when compared to either P2Y12−/− or C57BL/6J mice, further substantiating our finding that mice with CX3CR1 loss have the most distinct proteome (Fig. 1C). Different proteins and biological processes were found through differential expression analysis than those found through WPCNA and correlation analysis, identifying unique proteomic signatures tied to specific genotype comparisons. This highlights the benefit of using multiple bioinformatic methods to robustly characterize proteomes.

2.8. *Radiation-induced changes in cortical protein expression differ with genetic deficiencies in microglial signaling pathways*

Changes in the brain following radiation are regulated by microglial signaling pathways in other models (Jenrow et al., 2013; Markarian et al., 2021; Hinkle et al., 2019, 2023; Xu et al., 2015, 2016). However, no studies to date have examined whether deficiencies in P2Y12 and CX3CR1 signaling regulate radiation-induced changes in the cortical proteome. We first evaluated whether co-expression modules linked to radiation exposure from our WPCNA were regulated by genotype. We used a linear model followed by ANOVA to assess the impact of genotype, sex, radiation exposure, and their interactions on MEs (Supplemental Fig. 5A). There was weak evidence of an interaction between genotype and radiation for the black and turquoise MEs, but a significant interaction between sex, genotype, and radiation exposure for the red ME and the tan ME (Supplemental Figs. 5A,D,E). However, post-hoc analysis revealed no significant differences between irradiated and control mice within genotype or within genotype and sex (Supplemental Figs. 5B–E), suggesting radiation-induced changes in co-expression modules identified in our WPCNA did not significantly differ by sex or genotype.

To identify specific proteins whose radiation-induced changes in expression were affected by changes in microglial signaling, we used a linear model followed by ANOVA to identify 530 proteins with a significant interaction between genotype and radiation exposure. From there, we identified 185 proteins whose radiation-induced changes in expression were dependent on genotype, specifically examining differences between irradiated and control mice within each genotype. Eleven of these proteins had effects that were sex-dependent (ANOVA BH corrected p-value$<$0.05 for the interaction between sex, genotype, and radiation exposure followed by Tukey's post hoc comparisons p-value $p < 0.05$, specifically examining differences between irradiated and control mice within each genotype and within each sex). This left 174 proteins whose radiation-induced changes in expression were genotype, but not sex, specific (Fig. 6A). Of these proteins, 103 proteins were specifically altered between irradiated and control C57BL/6J mice. 9 proteins changed with radiation in C57BL/6J mice and either P2Y12−/− or CX3CR1−/− mice. Five proteins were altered in both C57BL/6J mice and CX3CR1−/− mice with irradiation, but not P2Y12−/− mice, including Dctn1, Sash1, Cltc, Camsap3, and P2Y12. Four proteins were altered in both C57BL/6J mice and P2Y12−/− mice with irradiation, but not CX3CR1−/− mice, including Selenbp1, Nt5c2, Phgdh, and Wasf2. Gene ontology enrichment analysis revealed the 112 proteins altered between irradiated and control C57BL/6J mice were associated with biological processes involving synapses and neuronal cellular components (Fig. 6A and B). This result may reflect the synaptic loss and altered neuronal function following radiation exposure shown in other models (Hinkle et al., 2019; Parihar et al., 2013; Zhang et al., 2018, 2020). The top 5 proteins whose expression was changed following radiation in C57BL/6J mice and differed by genotype were P2Y12, Mrps24, Rap1gap.Rap1gap2, Acss1, and Wasf2 (lowest Tukey's post hoc comparison p-value, Fig. 6E–I). Mrps24 and Acss1 were downregulated and Rap1gap.Rap1gap2 was upregulated only in C57BL/6J mice following radiation. Wasf2 was downregulated with irradiation in both

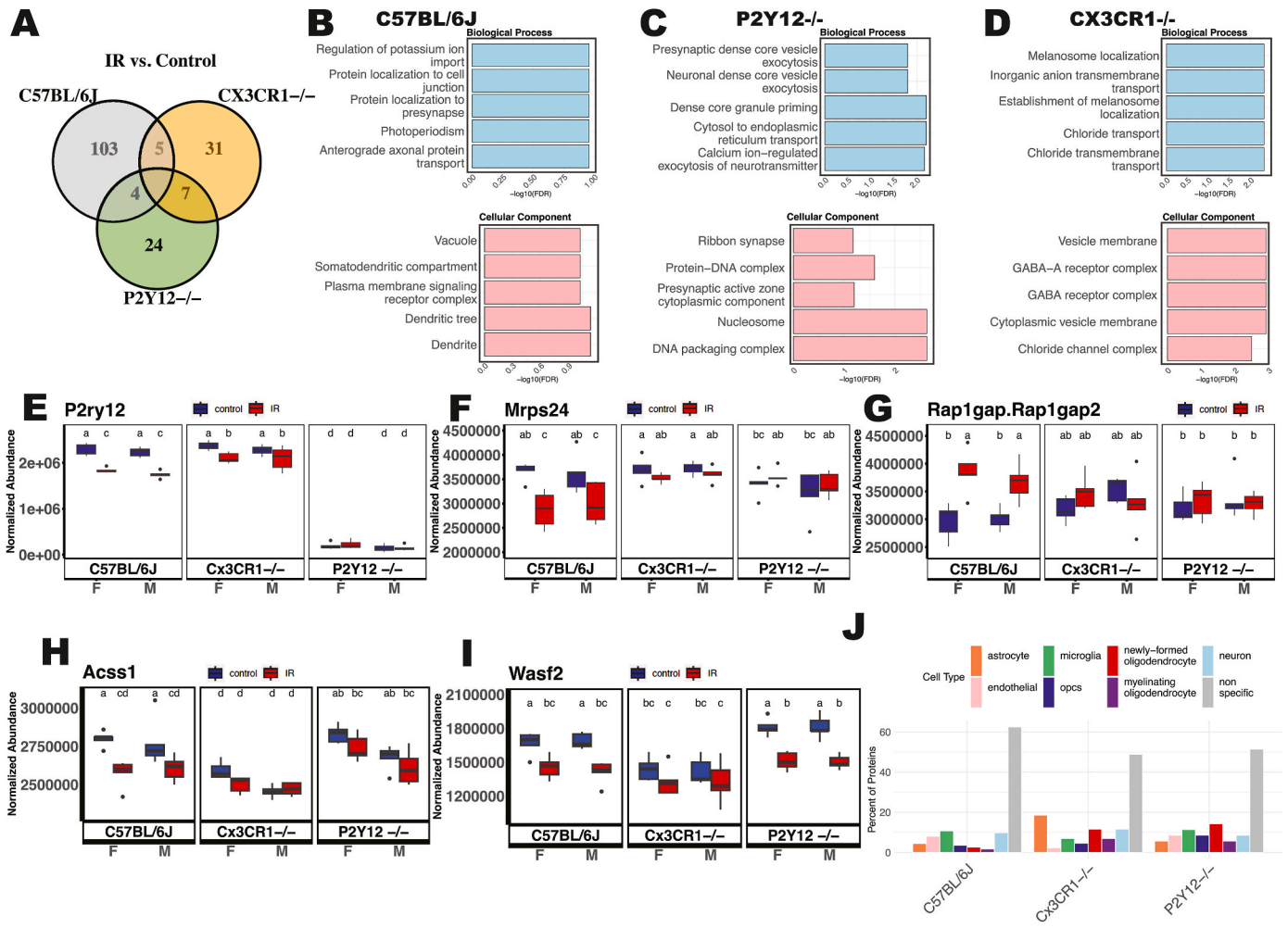

Fig. 6. Identification of genotype-dependent proteomic expression changes between irradiated and control mice. A linear model followed by ANOVA was used to identify 530 proteins with a significant interaction between genotype and radiation exposure (ANOVA BH-corrected p-value<0.05). From there, Tukey's post hoc comparisons (p-value <0.05) was used to identify 185 proteins with differences between irradiated and control mice within each genotype. A) Venn diagram showing the number of proteins with significantly changed expression between irradiated and control C57BL/6J, P2Y12−/− and CX3CR1−/− mice, as well as overlapping proteins. Biological processes (top; blue) and cellular components (bottom; pink) associated with proteins that were specifically changed between irradiated and control C57BL/6J B), P2Y12−/− C) and CX3CR1−/− D) mice. The top 5 proteins (lowest Tukey's post hoc comparison p-value) whose expression was altered in C57BL/6J mice with irradiation and were dependent on genotype were P2RY12, Mrps24, Rap1gap.Rap1gap2, Assc1, and Wasf2 (E–I). Significance was determined by a linear model followed by ANOVA and Tukey's post hoc testing ($p < 0.05$). J) The percent of proteins with significantly changed expression between irradiated and control C57BL/6J, P2Y12−/− and CX3CR1−/− mice for the following cell types: astrocytes, endothelial cells, microglia, oligodendrocyte progenitor cells (OPCs), newly-formed oligodendrocytes, myelinating oligodendrocytes, neurons, or nonspecific. N = 5 mice per sex/group/genotype. Radiation exposure is abbreviated as IR. False Discovery Rate is abbreviated as FDR.

C57BL/6J and P2Y12−/− mice, but not CX3CR1−/− mice. P2Y12 was downregulated in irradiated C57BL/6J and CX3CR1−/− mice (Fig. 6E), aligning with previous reports of decreased P2Y12 expression in irradiated hippocampal microglia isolated from wild type female mice (Osman et al., 2020). Most of the 112 proteins altered between irradiated and control C57BL/6J mice are not predominantly expressed by one cell type (non-specific, 62.5%, Fig. 6J). Of those that are predominantly expressed in certain cell types, most of were expressed by microglia (10.7%), or neurons (9.82%, Fig. 6J).

35 proteins were altered by irradiation in P2Y12−/− mice, with 24 proteins changing only between irradiated and control P2Y12−/− mice. Proteins altered by irradiation in P2Y12−/− mice were associated with biological processes involving exocytosis and cellular components involving DNA and synapses (Fig. 6A–C), and were largely not specific to a single cell type (non-specific, 51.4%, Fig. 6J). Cell-specific proteins were expressed by newly formed oligodendrocytes (14.3%), microglia (11.4%), and neurons (8.57%, Fig. 6J). 43 proteins were altered by irradiation in CX3CR1−/− mice, with 31 proteins being unique to this genotype. Proteins altered by irradiation in CX3CR1−/− mice were associated with biological processes involving ion transport and cellular components of GABA receptors (Fig. 6A–D), and 48.8% were not predominantly expressed by one cell type (non-specific, 48.8%, Fig. 6J). Cell-specific proteins were expressed by astrocytes (18.6%), neurons (11.6%) and microglia (6.89%, Fig. 6J). This may represent a sensitivity or possibly protective response of astrocytes to radiation specifically in CX3CR1−/− mice. Seven proteins were altered by irradiation in both P2Y12−/− and CX3CR1−/− mice, but not C57BL/6J mice, including Ncam1, Ass1, Bcan, Dglucy, Syngr3, Psat1, and Pex14 (Fig. 6A). Given that fewer proteins were altered by irradiation in P2Y12−/− and CX3CR1−/− mice (24 and 31, respectively) compared to C57Bl/6J mice (103), it is possible that loss of these microglial signaling pathways confers some resistance to radiation exposure. Collectively, these result show radiation-induced changes in protein expression differ in mice with genetic deficiencies in microglia signaling pathways.

2.9. Radiation-induced changes in cortical protein expression differ by sex and genotype

As males and females can display different radiation responses, we also wanted to determine whether radiation-induced changes in cortical proteomic expression differed by sex and genotype (Hinkle et al., 2019, 2023; Parihar et al., 2020). To identify proteins whose radiation-induced changes in expression differed among both sex and genotype, we used a linear model followed by ANOVA to identify 321 proteins with a significant interaction between sex, genotype, and radiation exposure (ANOVA BH corrected p-value<0.05). From there, we identified 45 proteins whose radiation-induced changes in expression differed among sex and genotype (Tukey's post hoc comparisons p-value <0.05, specifically examining differences between irradiated and control mice, within each genotype, within each sex, Fig. 7A and B). Of these, most protein expression changes were between irradiated and control CX3CR1−/− mice (Fig. 7A and B), with 19 proteins changed in males and 4 changed in females. In C57BL6/J mice, radiation altered the expression of 13 proteins in females and two proteins (Alkbh5 and Mrps11) in males. In P2Y12−/− mice, 4 proteins (Vps13d, Mocs2, Ovca2, and Dcps) were changed in males, and two (Safb2 and Wdr7) in females. Overall, these findings identify a subset of proteins whose

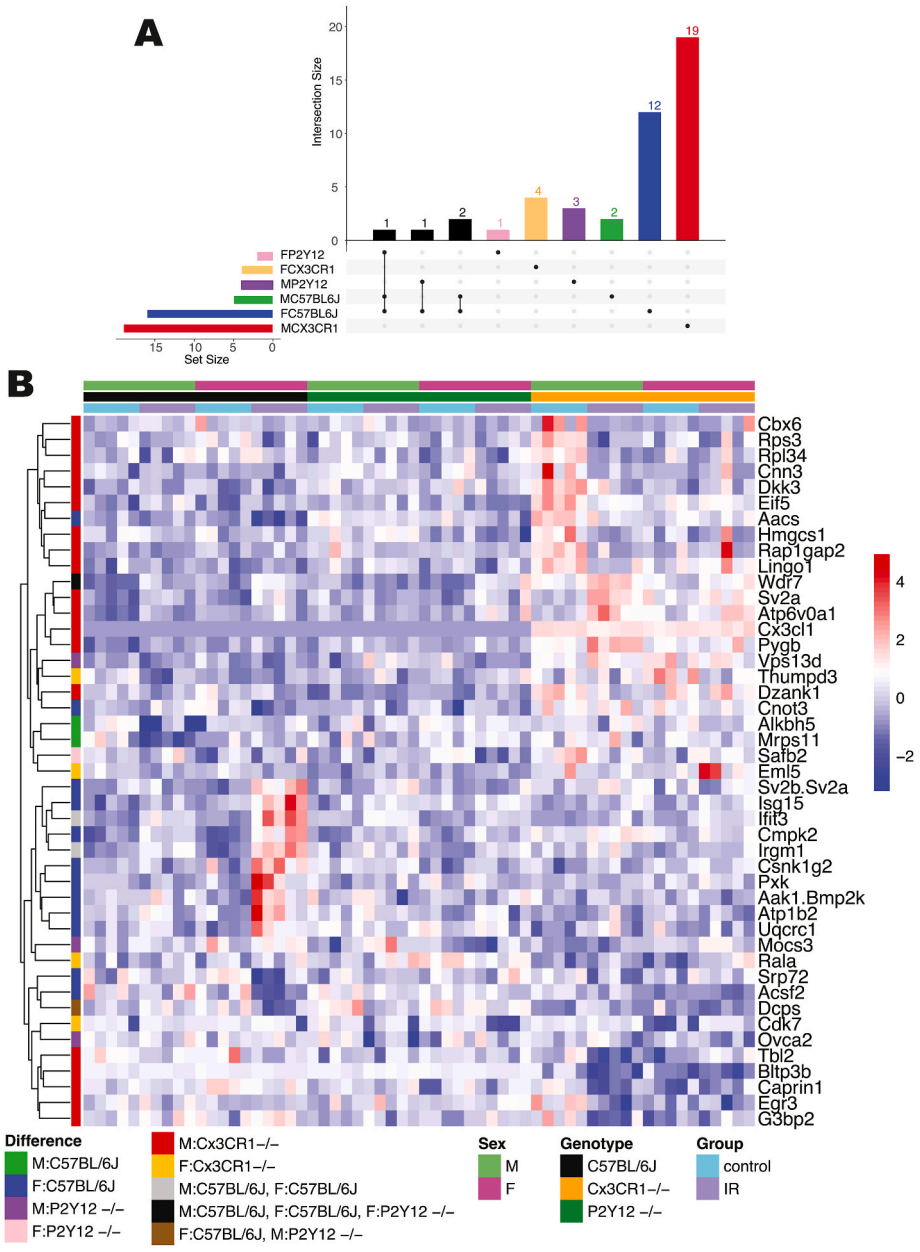

Fig. 7. Identification of sex and genotype-dependent proteomic expression changes between control and irradiated mice. A linear model followed by ANOVA was used to identify 321 proteins with a significant interaction between genotype and radiation exposure (ANOVA BH-corrected p-value<0.05). From there, Tukey's post hoc comparisons (p-value <0.05) was used to identify 45 proteins with differences between irradiated and control mice within each genotype, within each sex. A) Upset plot showing the number of proteins with significantly changed expression between irradiated and control male and female C57BL/6J, P2Y12−/−, and CX3CR1−/− mice. The number of proteins that were altered by irradiation are shown on the y-axis for each comparison. Black dots underneath the bars reflect the corresponding comparison. Multiple dots are present under bars where proteins were changed by irradiation for multiple comparisons. Set size is the number of proteins that differed for each denoted comparison. B) Heatmap showing the 45 proteins whose expression was dependent on sex and genotype. The horizontal legend shows sample information, whereas the vertical legend shows which samples were significantly different in that row. N = 5 mice per sex/group/genotype. Radiation exposure is abbreviated as IR.

radiation-induced changes in expression differed by both sex and genotype.

2.10. Locomotive behavioral outcomes differ by genotype, sex, and radiation exposure

Alterations in behaviors following radiation are reported in rodent models, with many showing response differ among males and females (Hinkle et al., 2023; Parihar et al., 2020; Krukowski et al., 2018b; Liu et al., 2019; Roughton et al., 2012). Furthermore, mice with deficiencies in receptors critical for microglia-neuronal communication or injury response exhibit altered behavioral responses to radiation (Kalm et al., 2016; Markarian et al., 2021; Xu et al., 2015; Belarbi et al., 2013; de Guzman et al., 2022). Some of these changes are also reported to be sex-dependent, demonstrating an interaction effect between sex and genotype (de Guzman et al., 2022). We therefore sought to determine how sex, radiation exposure, deficiencies in CX3CR1 and P2Y12, and their interactions impact behavioral outcomes. Before collecting tissue for the proteomic analysis described above, we performed the open field test (OFT) to assess locomotor activity of adult male and female C57BL/6J, P2Y12−/− and CX3CR1−/− IR and control mice. By using a linear model followed by ANOVA, we examined the effects of genotype, sex, radiation exposure, and their interactions on behavioral outcomes (Table 1&2).

For the OFT, we first examined behavioral outcomes from the whole session (OFT:WS), finding sex had the strongest impact on most behavioral outcomes, followed by genotype (Fig. 8A). Indeed, principal component analysis of behavioral outcomes revealed a visible distinction between males and females (Fig. 8B). For ambulatory activities and resting time, there was a main effect of genotype (Table 1). Post hoc analysis revealed P2Y12−/− mice had greater ambulatory time, counts, distance, and episodes compared to CX3CR1−/− mice, as well as lower resting time compared to C567Bl/6J mice and CX3CR1−/− mice (Fig. 8C, Supplemental Figs. 8A–C). There was a trend towards higher ambulatory counts and episodes in P2Y12−/− mice compared to C567Bl/6J mice as well, though this did not reach statistical significance ($p < 0.1$). Additionally, there was a significant interaction between sex and genotype for the average speed and total speed of ambulatory episodes (Table 1; Supplemental Figs. 8D and E). Post hoc analysis revealed P2Y12−/− males had significantly higher average and total speed during ambulatory episodes than P2Y12−/− female mice. Overall, these findings suggest P2Y12−/− mice have increased ambulatory activity, with P2Y12−/− males specifically exhibiting increased ambulatory activities for some outcomes.

Examining stereotypic activity, we found a significant main effect of sex (Table 1; Fig. 8D), where males had greater stereotypic counts and time. There was a significant interaction between sex and genotype for vertical time and counts (Table 1; Fig. 8E). Post hoc analysis revealed significant differences in vertical time between sexes among all genotypes, with P2Y12−/− males exhibiting the highest and CX3CR1−/− females exhibiting the lowest vertical time. For jump time and counts, there was a main effect of sex, genotype, and radiation, but not their interactions (ANOVA p-value<0.05; Table 1; Fig. 8F). Males had significantly lower jump time and counts than females and P2Y12−/− mice had higher jump time and jump counts than C57BL/6J and CX3CR1−/− mice. Irradiated mice had lower jump time and jump counts than control mice. Overall, these results indicate that genotype and sex had a significant impact on most locomotor outcomes, while the effects of radiation were minimal.

As sex had an overwhelming impact on ambulatory behavior in the OFT:WS and behavioral outcomes in mice are often sex-dependent, we decided to further examine behavioral outcomes in the OFT for males and females separately, as well as both sexes combined (Table 2). This analysis allowed us to assess locomotive behavior with respect to time (OFT:TC), where each bin represents a 5-min interval. We used a repeated-measures linear mixed-effects model followed by ANOVA and

Table 1
Summary of statistical outcomes from the open field test (whole session) and elevated plus maze. A linear model followed by ANOVA was used for statistical analysis. Bolded ANOVA p-values are <0.05. All other listed ANOVA p-values are <0.1. Factors not listed had ANOVA p-values >0.1. Radiation exposure is abbreviated as IR.

Behavioral Outcome	Factor	F Ratio	ANOVA P-value
OFT: Whole Session			
Ambulatory Counts	Genotype	7.11851427	**1.26E-03**
	Sex X Genotype	3.02104403	5.30E-02
Ambulatory Distance	Genotype	5.3074574	**6.36E-03**
Ambulatory Episodes	Genotype	4.68400326	**1.12E-02**
Ambulatory Episodes Average Speed	Sex X Genotype	6.14377284	**2.99E-03**
	Genotype X Radiation	2.43674241	9.23E-02
Ambulatory Episodes Total Speed	Genotype	3.39127939	**3.74E-02**
	Sex X Genotype	4.72718945	**1.08E-02**
Ambulatory Time (sec)	Genotype	5.59481688	**4.90E-03**
Jump Counts	Sex	69.442362	**3.06E-13**
	Genotype	7.94084617	**6.12E-04**
	Radiation	6.40432945	**1.29E-02**
	Sex X Genotype	2.50813061	8.62E-02
Jump Time (sec)	Sex	59.2358873	**7.69E-12**
	Genotype	16.7361791	**4.82E-07**
	Radiation	4.61522285	**3.40E-02**
Resting Time (sec)	Genotype	8.86252905	**2.76E-04**
Stereotypic Counts	Sex	22.243436	**7.36E-06**
Stereotypic Time (sec)	Sex	50.2496466	**1.57E-10**
Vertical Counts	Sex	10.1789426	**1.87E-03**
	Genotype	15.7003554	**1.07E-06**
	Sex X Genotype	4.34879964	**1.53E-02**
Vertical Time (sec)	Sex	56.1138939	**2.15E-11**
	Genotype	26.2989927	**5.31E-10**
	Sex X Genotype	5.37653271	**5.97E-03**
Elevated Plus Maze			
Mean Duration in Center (s)	Genotype	10.0328348	**1.06E-04**
	Sex X Genotype X Radiation	4.15024889	**1.85E-02**
Mean Duration in Closed (s)	Genotype	7.50309031	**9.16E-04**
	Sex X Genotype	4.85880768	**9.67E-03**
	Sex X Radiation	2.86640201	9.35E-02
Mean Duration in Open (s)	Genotype	11.0671843	**4.51E-05**
Percent Entries in Open	Sex	10.5243946	**1.60E-03**
	Genotype	33.3734603	**7.47E-12**
Percent Entries in Closed	Sex	10.5243946	**1.60E-03**
	Genotype	33.3734603	**7.47E-12**
Percent Time in Center Hub	Genotype	15.1625378	**1.74E-06**
	Genotype X Radiation	2.39762036	9.61E-02
	Sex X Genotype X Radiation	3.63427718	**2.99E-02**
Percent Time in Closed	Sex	3.02134703	8.52E-02
	Genotype	32.4187614	**1.33E-11**
	Genotype X Radiation	2.52010411	8.55E-02
	Sex X Genotype X Radiation	2.45264596	9.12E-02
Percent Time in Open	Sex	3.13511846	7.96E-02
	Genotype	26.139729	**7.10E-10**
Ratio of Open to Closed Entries	Sex	10.3497822	**1.74E-03**
	Genotype	32.6503342	**1.16E-11**
Ratio of Open to Closed Time	Genotype	25.047614	**1.47E-09**
Time in Center	Genotype	14.0580973	**4.11E-06**
	Genotype X Radiation	2.47054042	8.96E-02
	Sex X Genotype X Radiation	3.76082299	**2.66E-02**
Time in Closed	Genotype	33.6336411	**6.39E-12**
	Sex	3.16997481	7.80E-02
Time in Open	Genotype	26.1326209	**7.13E-10**
Total Closed Entries	Genotype	4.16901454	**1.82E-02**
	Sex X Genotype	5.08818875	**7.85E-03**
	Sex X Radiation	3.31881958	7.15E-02
Total Entries	Genotype	10.8992514	**5.18E-05**
	Sex X Genotype	3.79934581	**2.57E-02**

(*continued on next page*)

Table 1 (*continued*)

Behavioral Outcome	Factor	F Ratio	ANOVA P-value
Total Open Entries	Sex	8.55611075	**4.25E-03**
	Genotype	30.3157736	**4.87E-11**

found several behavioral outcomes were impacted by genotype, radiation, bin, or their interactions (Table 2). Unsurprisingly, as animal ambulatory behavior in the OFT changes over time (Sobolewski et al., 2020), bin had the strongest impact on all behavioral outcomes in the OFT:TC for females, males and both sexes combined (Fig. 9A–C). Genotype had the second strongest impact on behavior for all sexes and combinations, mirroring the results from the OFT:WS analysis. When combining sexes, PCA analysis showed a distinction between bin 1 and the rest of the timepoints (Fig. 9D), while genotype and radiation showed relatively little distinction (Fig. 9E and F). Regarding radiation exposure, we found a significant interaction between bin, radiation exposure, and genotype on ambulatory counts and ambulatory time in male mice, as well as a main effect of radiation on ambulatory episode average speed and jump counts in female mice (Table 2). These findings support the conclusion that sex and genotype have a stronger influence on locomotor behaviors compared to radiation in our model, but also show some radiation effects when separating by sex and examining outcomes over time.

2.11. *Reduced exploratory behaviors are linked to genetic deficiencies in microglial signaling pathways*

We next performed the elevated plus maze (EPM) to examine exploratory behavioral outcomes. By using a linear model followed by ANOVA, we examined the effects of microglial signaling, sex, and radiation exposure on behavioral outcomes (Table 1). Genotype had the strongest impact on EPM behavior (Fig. 10A), with PCA analysis indicating a subtle shift between C57BL6/J mice and both P2Y12 −/− and CX3CR1−/− mice (Fig. 10B). There was also a significant interaction between sex, genotype, and radiation exposure (Table 1) on the percent time (Fig. 10C) and mean duration (Supplemental Fig. 9A) in the center hub. However, post hoc analysis did not show significant differences with radiation exposure in males or females of any genotype.

There was a significant main effect of genotype (Table 1) on the percent time (Fig. 10D and E), mean duration, and total entries into the open and closed arms (Supplemental Figs. 9B–E), suggesting exploratory behaviors differ among genotypes. For the EPM, more time spent in the open arms relative to the closed arms is indicative of greater exploratory

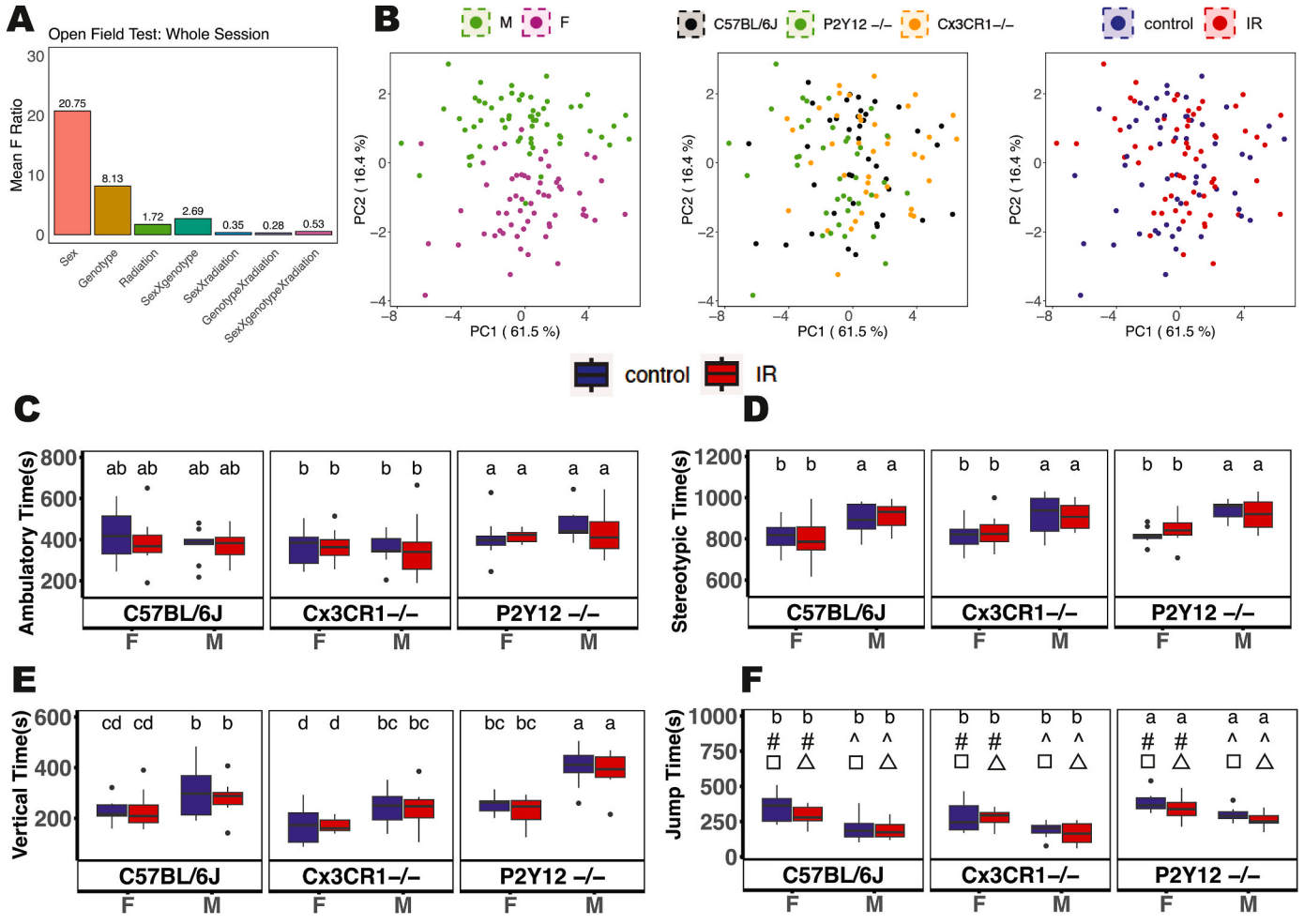

Fig. 8. Behavioral Outcomes in the Open field test: whole session (OFT:WS) are regulated by sex, genotype, and radiation exposure. A) The effects of sex, genotype, radiation exposure and their interactions on behavioral outcomes in the OFT:WS. B) Sample variation revealed by PCA analysis color-coded by sex, genotype, and radiation exposure. C-F) Locomotive behavioral outcomes across sex (males and females), genotype (C57BL/6J, CX3CR1−/−, P2Y12−/−) and radiation exposure (IR and control). The top and bottom lines in the box plots represent the upper and lower quartile values, and the center lines represent the median. Group means with the same letter, symbol, or shape are not significantly different, whereas group means with different letters, symbols, or shapes are significantly different. Significance was determined by a linear model followed by ANOVA and Tukey's post hoc testing ($p < 0.05$). N = 9–11 mice per sex/group/genotype. Radiation exposure is abbreviated as IR. PC stands for Principal Component.

Table 2
Summary of statistical outcomes from the open field with respect to time. A linear model followed by ANOVA was used for statistical analysis. Radiation exposure is abbreviated as IR. Listed factors have a p-value<0.05. ~ indicates p-value <0.1.

Open Field Test: Time course			
Behavioral Outcome	Male	Female	Combined (Male + Female)
Ambulatory Counts	Bin X IR X Genotype	Bin X Genotype	Bin X Genotype, ~Bin X IR X Genotype
Ambulatory Distance	Bin X Genotype, ~Bin X IR X Genotype	Bin X Genotype	Bin X Genotype
Ambulatory Episodes Average Speed	Bin, ~Bin X IR	IR, Bin X Genotype	IR, Bin X Genotype, ~Bin X IR, ~ IR X Genotype
Ambulatory Episodes	Bin X Genotype, ~Bin X IR X Genotype	Bin	Bin X Genotype
Ambulatory Episodes Total Speed	Bin X Genotype	Bin	Bin X Genotype
Ambulatory Time	Bin X IR X Genotype	Bin X Genotype	Bin X Genotype
Jump Counts	Bin, Genotype	Bin, IR, ~Bin X Genotype	Bin, Genotype, ~IR
Jump Time	Bin, Genotype	Bin X Genotype, ~Bin X IR	Bin X Genotype
Resting Time	Bin, Genotype	Bin X Genotype	Bin X Genotype
Stereotypic Counts	Bin X Genotype	Bin X Genotype	Bin X Genotype
Stereotypic Time	Bin X Genotype	Bin X Genotype	Bin X Genotype
Vertical Counts	Bin X Genotype	Bin, Genotype	Bin X Genotype
Vertical Time	Bin X Genotype	Bin, Genotype	Bin X Genotype

behavior in rodents, as they naturally prefer enclosed spaces. There was a main effect of genotype on the ratio of time spent in the open to closed arms, (Table 1, Fig. 10F), with CX3CR1−/− and P2Y12−/− mice −/− spending relatively less time in the open arms compared to C57BL/6J mice. For the ratio of open to closed entries, there was a significant main effect of genotype and sex (Table 1, Fig. 10G). Both CX3CR1−/− and P2Y12−/− mice had a lower number of entries into the open arm relative to the closed arm compared to C57BL/6J mice, with CX3CR1−/− mice exhibiting the lowest ratio of open to closed entries. Females also had a higher number of entries into the open arm relative to the closed arm compared to males. In summary, these findings suggest mice with genetic deficiencies in CX3CR1 and P2Y12 signaling exhibit reduced exploratory behavior.

3. Discussion

Microglial signaling pathways are of interest in the context of radiation injury, where microglia are believed to mediate changes in structure and function. Sex differences in responses to radiation are also important to consider when modeling radiation effects. Here, we performed a comprehensive analysis of the cortical proteomes from irradiated and control C57BL/6J, P2Y12−/−, and CX3CR1−/− mice of both sexes, coupled with measurements of locomotive and exploratory behaviors. We show proteomic profiles and exploratory behaviors mostly differed by genotype, while locomotor behavior mostly differed by sex (Fig. 11). We utilized multiple bioinformatics methods to identify proteins and biological processes associated with different experimental conditions. Our findings provide novel insights into the biological processes and proteins strongly linked to microglial P2Y12 and CX3CR1 signaling, sex, radiation exposure, and their interactions.

3.1. Mice with loss of microglial signaling receptors have distinct proteomes and behavioral profiles

To our knowledge, there has been no comprehensive analysis on either P2Y12−/− or CX3CR1−/− mice cortical proteomes. We therefore provide new insights into proteins and biological pathways that are associated with these genotypes with respect to one another, and with respect to C57BL/6J controls. We found most variation between proteomes was attributable to the CX3CR1−/− genotype, with differences observed in metabolic and synaptic biological processes, in line with the role of CX3CR1 signaling in orchestrating responses to injury and synaptic development (Camacho-Hernandez et al., 2023). We found that Cx3Cl1, the ligand for CX3CR1, was highly upregulated in CX3CR1−/− mice, illustrating a potential compensatory mechanism of the CX3CL1/CX3CR1 axis. A previous study using RNA-sequencing of hippocampal tissue from CX3CR1−/− mice compared to wild type mice found transcriptional differences in immune regulation, cell growth, proliferation, and migration (Rimmerman et al., 2017). We identified biological processes associated with CX3CR1 related to metabolism and synapses (synaptic signaling, anterograde, trans synaptic signaling, chemical synaptic transmission, oxoacid metabolic processes, carboxylic acid metabolic processes, and small molecule metabolic processes), which could highlight regional differences in the adaptation to CX3CR1 loss between the hippocampus and cortex.

Given the important role of P2Y12 in microglial function both during homeostasis and pathology (Lin et al., 2020), it is surprising that P2Y12−/− mice did not show as many changes in their proteome as CX3CR1−/− mice when compared to C57BL/6J mice. Loss of P2Y12 resulted in changes in pathways governing cytoplasmic translation, suggesting that P2Y12 signaling may be involved in subcellular regulation of local protein synthesis within microglia. In fact, P2Y12 is likely to be locally translated (Vasek et al., 2023) and further experiments on local microglial translation in P2Y12−/− mice might elucidate its role in this process. Loss of P2Y12 also impacted metabolic pathways, especially those involving Acetyl-CoA. Given the strong impact of reactive state on microglial metabolism (Fairley et al., 2021) and the high expression of P2Y12 in homeostatic microglia, this may suggest that P2Y12 expression regulates microglial metabolism in a way that relates to the demands of the roles of microglia in homeostasis versus pathology.

We also found that genotype had the strongest impact on behavior in the EPM, suggesting genetic deficiencies in canonical microglial signaling pathways are linked to alterations in exploratory behaviors. P2Y12−/− mice had a lower duration and number of entries in the open arms compared to C57BL/6J mice, mirroring the findings of others (Zheng et al., 2019; Peng et al., 2019). Previous reports show altered exploratory behaviors (Mendez-Salcido et al., 2022) or no impact of CX3CR1 deficiency on behaviors in the elevated plus maze (Rogers et al., 2011; Hellwig et al., 2016). In contrast, we found both the ratio of time spent and the number of entries in the open versus closed arms was decreased in P2Y12−/− and CX3CR1−/− mice compared to C57BL/6J mice. These results indicate alterations in exploratory behavior in both P2Y12 and CX3CR1 deficient mice, highlighting how deficiencies in microglia signaling by different mechanisms can impact cognitive function. Though exploratory behavior was altered in both P2Y12 and CX3CR1 deficient mice, proteomic differences were more robust in CX3CR1 deficient mice. Future experiments examining more complex behaviors could uncover behavioral changes that are specific to CX3CR1−/− mice and possibly relate those behaviors to the biological processes which were altered in our proteomic analysis.

3.2. Radiation impacts cortical protein expression with limited effects on behavior

As cancer therapies improve, the surviving population grows, increasing the importance of understanding possible mechanisms

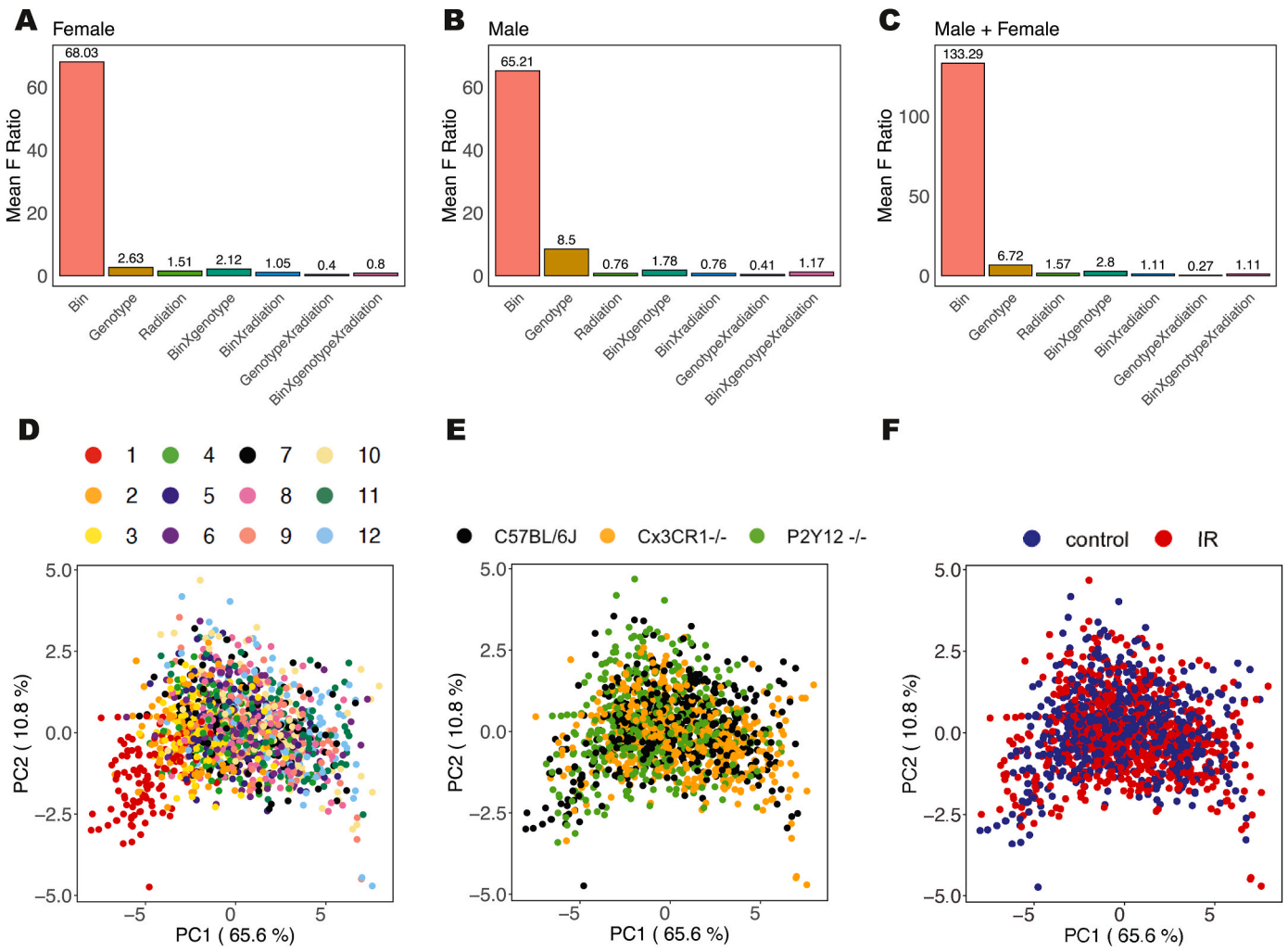

Fig. 9. Behavioral Outcomes in the Open field test: Time course (OFT:TC) are regulated by bin, genotype, and radiation. OFT data was analyzed in 5-min intervals, or "bins". The effects of bin, genotype, radiation exposure and their interactions on behavioral outcomes in the OFT:WS in females A), males B), and combining both sexes C). Sample variation revealed by PCA analysis color-coded by bin D), genotype E), or radiation exposure (F). Radiation exposure is abbreviated as IR. PC stands for Principal Component.

underlying radiation-induced cognitive decline. Previous studies have concentrated on the effects of radiation on the hippocampus and neurogenesis, reporting dysregulated microglial function and synaptic loss (Hinkle et al., 2019, 2023; Osman et al., 2020; Parihar et al., 2013; Monje et al., 2002; Raber et al., 2004). In agreement with these results, our study found immune and synaptic biological processes were impacted by irradiation, further demonstrating the vulnerability of the cortex to cranial irradiation exposure. Indeed, reports of deficits in cortical plasticity in mice following radiation exposure have been reported (Zhang et al., 2018). We also identified cortical proteins associated with radiation exposure whose RNA transcripts were reported to be impacted by radiation in the hippocampus, including those in the complement pathway (Markarian et al., 2021) and several microglial proteins (Hexb, Rsg10, Crybb1, Ctss, Ephx1 and Ifit3) (Osman et al., 2020). We found astrocytic Gfap, which previously was identified to increase in expression with radiation in the hippocampus (Moravan et al., 2011), was similarly increased with radiation exposure in the cortex. While most of the changes in expression we identified were relatively small, the fact that they agree with those reported using other methods, suggests that radiation damage may be mediated through similar mechanisms (glial activity and synapse loss) in different brain areas. Furthermore, our changes in protein expression in irradiated mice correlated with RNA expression levels of normal-appearing non-tumor brain tissue from glioblastoma (GBM) patients treated with radiation therapy. Differences between our results and observations from Ainslie et al. could be due to the temporal response of radiation therapy, gene to protein differences, or human to mouse differences. For example, we found complement protein C1QA downregulated, while Ainslie et al., found C1QA was upregulated. In mice, expression of complement proteins can increase or decrease depending on the time elapsed since irradiation (Markarian et al., 2021), which could explain the differences in directionality between our results.

While we only assayed two behavioral modalities - the OFT and EPM - our analyses suggested that radiation had limited effects on these behaviors compared to sex and genotype. The only significant main effect of radiation exposure on behavioral outcomes in the OFT for the whole session was jumping behavior, where radiation exposure reduced jump time and jump counts. We found no main effect of radiation on ambulatory behaviors for the OFT-WS, consistent with previous findings at 1-month post-radiation exposure, where no differences in the total distances traveled were observed between control and irradiated mice (Parente et al., 2020). We also found no significant effects of radiation on exploratory behaviors in the EPM. Previous reports in the literature using this test are mixed. At 12 days post irradiation, Tome et al. found no change in exploratory behavior in the EPM (Tome et al., 2015), while Njamnshi et al. (2020) found a decrease in time spent in the open arms,

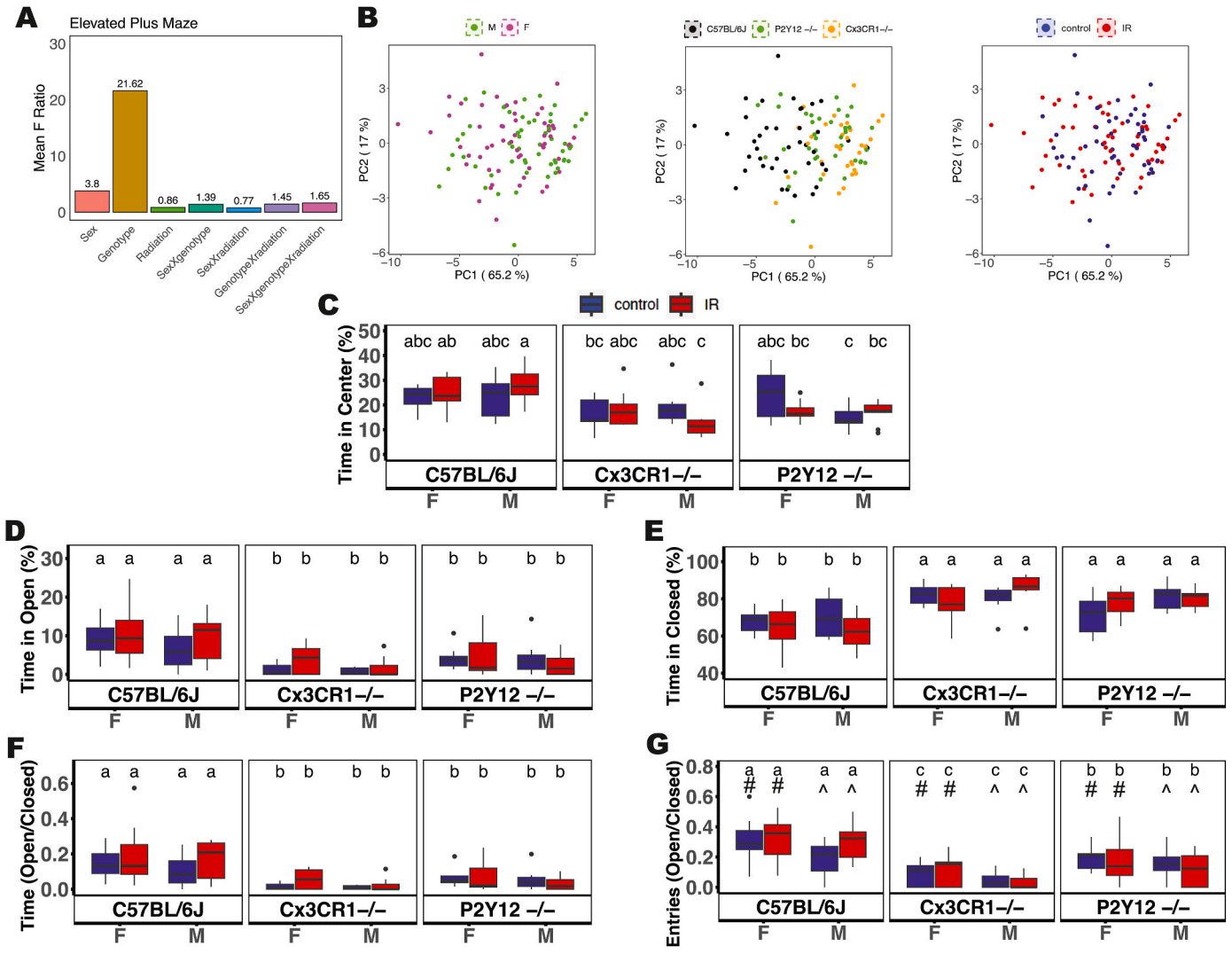

Fig. 10. Behavioral Outcomes in the Elevated Plus Maze (EPM) are regulated by sex and genotype, but not radiation. A) The effects of sex, genotype, radiation exposure and their interactions on behavioral outcomes in the EPM. B) Sample variation revealed by PCA analysis color-coded by sex, genotype, and radiation exposure. C-G) Anxiolytic behavioral outcomes across sex (males and females), genotype (C57BL/6J, CX3CR1−/−, P2Y12−/−) and radiation exposure (IR and control). The top and bottom lines in the box plots represent the upper and lower quartile values, and the center lines represents the median. Letters above box plots are generated from Tukey's HSD tests for ease of identifying differences across sex, genotype, and radiation exposure. For G) Letters represent significant genotype differences and #,^ represent sex differences. Group means with the same letter or symbol are not significantly different, whereas group means with different letters or symbols are significantly different. Significance was determined by a linear model followed by ANOVA and Tukey's post hoc testing ($p < 0.05$). N = 7–11 mice per sex/group/genotype. Radiation exposure is abbreviated as IR. PC stands for Principal Component.

with a trend starting around 3 weeks post-irradiation. Because molecular effects can often be detected earlier than apical effects, it is possible that the proteomic changes we describe precede changes in behavior. In line with this, the number of entries into the open arm were reported to increase at 120 days post cranial irradiation (Constanzo et al., 2020), but decrease at 3 months (Lee et al., 2022) and 6 months (Montay-Gruel et al., 2021) post irradiation exposure. Collectively, our findings indicate proteomic changes may precede gross behavioral changes following radiation exposure.

3.3. *Genetic deficiencies in Cx3CR1 and P2Y12 regulate radiation-induced proteomic expression*

As our findings and those of others strongly suggest glia are impacted by radiation, it is important to examine microglial signaling pathways as a therapeutic target throughout the brain. In response to insults, microglia respond to chemotactic signals to migrate towards site of injury, identify damaged components of their environment, and phagocytose damaged cells and debris (Yu et al., 2022). Microglial signaling pathways are known to govern radiation responses through regulation of microglial survival, chemotaxis, and phagocytic activity. For example, targeting components of the complement pathway can attenuate radiation-associated neurological deficits and neuroinflammatory changes (Kalm et al., 2016; Markarian et al., 2021; Hinkle et al., 2019, 2023). The purinergic receptors P2Y6 and P2X7 expression are both upregulated following radiation exposure and regulate microglial radiation responses (Xu et al., 2015, 2016). However, while P2X7 plays a role in mediating radiation-induced damage, P2Y6 may be neuroprotective against radiation injury (Xu et al., 2015, 2016). These studies offer compelling evidence that modulating microglial function can influence radiation responses within the brain. We identified proteins whose radiation-induced changes were dependent on P2Y12 and CX3CR1 signaling, providing further evidence that these pathways shape the proteome. Interestingly, loss of either microglial receptor reduced the effects of radiation on the cortical proteome suggesting that microglia modulate the brain's response to irradiation. Of the proteins

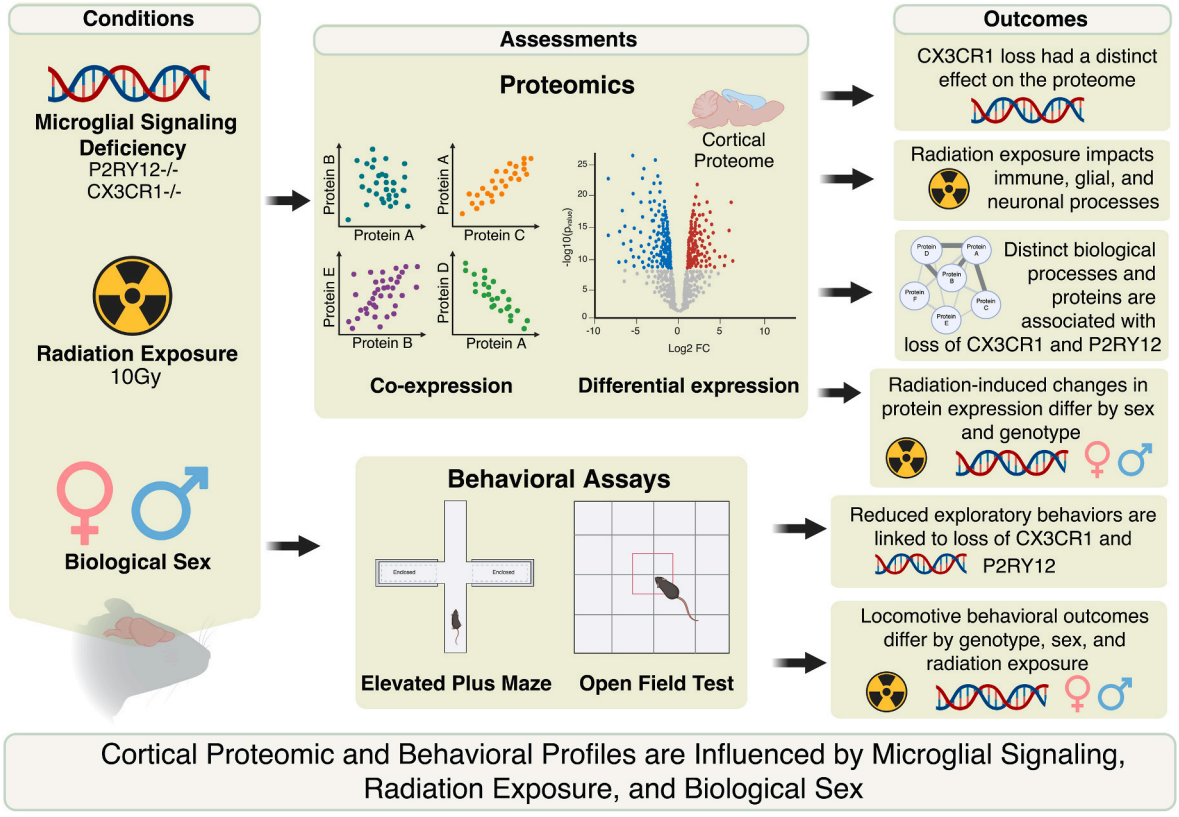

Fig. 11. Summary of experimental design and main findings.

altered by radiation in CX3CR1−/− mice that were predominantly expressed by a certain cell type, most were highly expressed in astrocytes, suggesting a potential role of CX3CR1 in regulating astrocytic responses to radiation exposure. Radiation-induced changes in CX3CL1 expression were also genotype dependent, with significant downregulation observed in male CX3CR1−/− mice with radiation exposure. Decreases in P2Y12 expression were also reported in both C57BL/6J mice and CX3CR1−/− mice exposed to radiation. Reports of changes in microglial P2Y12 expression following irradiation are somewhat controversial. Belcher et al., found no differences in P2Y12 protein levels at 48 h post irradiation with 20 Gy, whereas Osman et al. (2020), found decreases in P2ry12 transcript at 2- and 6-h post-irradiation with 8 Gy. Our results show differences in the expression of P2Y12 in cortical tissue in both males and females 1 month after irradiation, demonstrating a long-lasting impact of irradiation on this microglia homeostatic marker. This downregulation of P2Y12 could reflect a change in the reactivity of microglia after radiation exposure or could be the result of a radiation-driven loss of the microglial population (Whitelaw et al., 2021; Strohm et al., 2024). The radiation-induced changes in P2Y12 expression, also increase the importance of examining radiation-driven responses in the absence of P2Y12. Of the proteins altered between irradiated and control P2Y12−/− mice that are predominantly expressed in certain cell types, most were expressed by newly formed oligodendrocytes or microglia. This may indicate that P2Y12−/− deficiency causes newly formed oligodendrocytes or microglia to be more vulnerable to radiation exposure.

3.4. Implications of sex differences in proteomic expression and behavior on radiation responses

Biological sex is a risk factor for several neurodegenerative diseases (Levine et al., 2021), and can impact cognitive function in healthy adults (McCarrey et al., 2016; Jockwitz et al., 2021). As such the prevalence of cognitive disorders differs between males and females across different diseases. For example, there is a higher prevalence of Alzheimer's disease, major depressive disorder, and MS in females (Cao et al., 2020; Walton et al., 2020; Kessler et al., 2005), while Parkinson's disease, ALS, and ASD are more common in males (Baldereschi et al., 2000; Marras et al., 2018; Fontana et al., 2021; Goldblum et al., 2023). Furthermore, sex differences in microglia morphology, density, and transcriptional profiles exist throughout adolescence and into adulthood (Guneykaya et al., 2018; Hanamsagar et al., 2017; Thion et al., 2018; Villa et al., 2018; Schwarz et al., 2012), which could contribute to both the risk and progression of neurological disease. There is an ongoing need for understanding microglial contributions to sex differences in cognitive functioning and the underlying molecular pathways affected by biological sex. Sex can have a profound effect on gene expression and behavior through both genetic and hormonal mechanisms. Importantly, several of our findings regarding sex-differences support those from other behavioral models and brain areas that used RNA-based or histological methods. We identified proteins with higher expression in females, aligning with previous reports from others, including Hsp90aa1, Ddx3x, Eif2s3x, Prdx6 (Weis et al., 2021; Wingo et al., 2023; Weickert et al., 2009; Distler et al., 2020; Xu et al., 2006), as well as several that are X-linked (Eif2s3x, Ddx3x, Pbcd1). Fifty-seven of the cortical proteins we identified to have sex-biased expression were also identified by Wingo et al. (2023) as sex-biased in humans, two of which (Prdx6 and Fam81a) have been associated with schizophrenia. These findings bolster the hypothesis of inherent sex-based differences in protein composition between males and females.

3.5. Interaction effects between sex, genotype, and radiation exposure

Increasing evidence suggests males and females have differential sensitivity to radiation exposure (Hinkle et al., 2019, 2023). These differences could be in part due to subtle basal differences in tissue

structure and protein composition between males and females, as described above. In our analysis, we identified 45 proteins whose radiation-induced changes in expression were dependent on both sex and genotype. This provides some evidence of varying sensitivity to radiation exposure between males and females with and without canonical microglial signaling receptors.

As behavioral outcomes in mice are often sex-dependent (Sobolewski et al., 2020), we assessed behavioral outcomes of both males and females of our three genotypes. Though sex had the greatest impact on locomotive behaviors in the open field test, many of these effects were also dependent on genotype. The exception to this was stereotypic behaviors, which were greater in males than females regardless of genotype. We did observe sex and genotype dependent effects on ambulatory episode speed, vertical activity, and jumping activity that have not been previously reported to our knowledge, demonstrating how the interactions of these factors can shape behavior. Our analysis revealed that sex had a significant effect on locomotor behavior. However, we did not observe sex-specific differences in behavior after irradiation.

We did observe significant interactions between sex, genotype, and irradiation on endpoints in the center hub of the maze in the EPM. We also report weak evidence of an interaction between either radiation and sex, or radiation, sex, and genotype on behaviors in the closed arm, though none of these were significant. Furthermore, when separating by sex and analyzing by time intervals (bin) in the OFT, we found a significant interaction between bin, radiation exposure, and genotype on ambulatory counts and ambulatory time in male mice, as well as a main effect of radiation on ambulatory episode average speed and jump counts in female mice, suggesting these factors may shape ambulatory behavior differently in males and females. To our knowledge, there are no reports on how CX3CR1 or P2Y12 regulates behavior in the context of radiation injury with either the OFT or EPM. However, Wang et al. found a neuroprotective effect of exogenous fractalkine on microglia and found that fractalkine lentivirus treatment could ameliorate radiation-induced memory deficits in the Morris water maze, demonstrating the utility in targeting fractalkine in the context of radiation exposure (Wang et al., 2021). Some of our results in the EPM may be affected by differences in locomotor behavior that we described in OFT. However, the overall conclusions about the effects of sex, genotype, and irradiation appear to hold in measures that normalize for locomotion such as the percentage of time spent in open or closed arms.

3.6. Study limitations and future directions

Molecular pathways are commonly characterized by changes in gene-products through methods that assay RNA expression (Osman et al., 2020; Lee et al., 2022; Li et al., 2015). Consequently, little is known regarding effects of sex, microglia signaling, and radiation exposure on the brain proteome compared to the transcriptome (Wingo et al., 2023; Leszczynski, 2014). mRNA expression levels do not always correspond with protein levels because mRNA gene products undergo post-transcriptional and translational regulation, and there are different rates of degradation between mRNA and proteins (Wingo et al., 2023; Maier et al., 2009; Jung et al., 2017; Vogel et al., 2012; Sharma et al., 2015). Additionally, proteomic methods can identify proteins whose corresponding RNA gene products were not identified (Wingo et al., 2023; Jung et al., 2017; Vogel et al., 2012; Sharma et al., 2015), potentially identifying novel targets not detected using RNA-based methods. As such our study is novel in using a bioinformatics approach on the protein level to address radiation-induced changes in the context of altered microglial function. However, while our study provides novel insights into the interplay between sex, microglial signaling, and radiation exposures, several limitations must be discussed. Despite mass spectrometry being a powerful technique, one advantage of RNA-based methods is the ability to measure cytokine expression, which are not always reliably detected with proteomic methods (Stenken et al., 2015). Indeed, others have examined the RNA profiles of the brain after radiation in isolated microglia (Osman et al., 2020; Li et al., 2015) and whole tissue, demonstrating the neuroinflammatory impacts of irradiation. It is also important to note that the changes we identified in protein expression for both sex and radiation, though significant, were small (<2-fold), whereas those between genotypes were greater. We did however use a relatively low radiation dose, and it is plausible that the small changes we observed in the cortex would be more pronounced at higher radiation doses or at different timepoints. Our observations are also limited to the cortex, and basal and pathological changes in proteomic expression differ by brain region (Distler et al., 2020; Jung et al., 2017; Sharma et al., 2015), suggesting that proteomic studies should be performed in other brain areas. Though we did not determine the extent to which there may be infiltration of peripheral macrophages in our study, others have found no evidence of this at similar timepoints following irradiation with doses of 5, 8, or 10 Gy (Moravan et al., 2011, 2016; Han et al., 2016; Lee et al., 2013). In agreement with this, we did not detect peripheral macrophage markers CD163 and CCR2 in our proteomic profiling.

Additionally, the behavioral assessments we performed only provide insights in basic locomotor and exploratory behaviors, and it is likely that more complex memory and learning behaviors are impacted by the factors in our study. Though our study provides some evidence that microglial signaling through P2Y12 and Cx3CR1 may regulate behavior after radiation exposure, further studies are needed to determine whether targeting these pathways would be truly beneficial in combating radiation-induced cognitive decline. Moreover, as we only examined behavior at one timepoint, it is also possible that sex and genotype may impact radiation-induced changes in behavior at later or earlier timepoints post-irradiation. Therefore, further experimentation is needed to determine how sex, CX3CR1 and P2Y12 signaling, and radiation regulate the proteome and behavior differentially at other doses, timepoints and brain regions. Lastly, we used mice with global deficiencies of P2Y12 and CX3CR1. Although conditional microglial knockouts of P2Y12 largely replicate behavioral deficits of global P2Y12−/− mice (Peng et al., 2019), it is possible that there are developmental and systemic compensatory mechanisms which alter the biology of these mice and impact the interpretation of our results. Future experiments should therefore aim to provide more mechanistic insights into how these pathways regulate radiation responses by using pharmacological or temporally genetically controlled alterations in P2Y12 and CX3CR1 activity.

4. Methods

4.1. Animal husbandry

Experiments were performed in accordance with the University of Rochester Committee on Animal Resources according to National Institutes of Health Guidelines. All procedures involving animals were approved by the Institutional Animal Care and Use Committee (IACUC) at the University of Rochester. Wild type C57BL/6 (Jax Strain #:000664), CX3CR1−/− (Taconic Biosciences), P2Y12−/− (André et al., 2003) male and female mice 8–12 weeks old were used for the experiment. The latter two strains were maintained on a C57BL/6 background. All mice were exposed to 12 h of light and 12 h of dark and provided chow and water *ad libitum*. We estimated the sample size based on previous studies using similar analyses that detected significant differences in the parameters measured in our study (Sobolewski et al., 2020; Cubello et al., 2024; Merrill et al., 2022; Boeddrich et al., 2023; Shukla et al., 2015).

4.2. X-ray cranial irradiation

A small animal radiation research platform (SARRP) x-ray irradiator (225 kVp XStrahl) was used to perform computed tomography (CT) image guided whole-brain radiation therapy as previously described

(Whitelaw et al., 2021; Strohm et al., 2024). Briefly, mice were subjected a single 10 Gy dose from two parallel opposed beams using a 10 × 10 mm^2 beam collimator, given at 220 kV and 13 mA with a dose rate of 3.1 Gy/min, while under isoflurane anesthesia. Control mice were exposed to isoflurane and were not placed in the SARRP irradiator or exposed to radiation. A single dose of 10 Gy was chosen based on literature reporting cognitive deficits, transcriptional changes, and alterations of microglia dynamics in mice following a single dose of 8–10 Gy (Acharya et al., 2016; Allen et al., 2020; Markarian et al., 2021; Hinkle et al., 2023; Osman et al., 2020; Strohm et al., 2024; Bhat et al., 2020).

4.3. Open field test

Mice underwent behavioral testing from 32 to 36 days following cranial irradiation. Mice first underwent the open field test, followed by the elevated plus maze test. For the open field test, locomotor activity was examined in automated chambers equipped with 48-channel infrared photobeams (Med Associates) over an hour-long session. Photobeam breaks were recorded in 5-min bins resulting in 12 bins for the hour-long locomotor activity session. Horizontal, vertical, stereotypic, and ambulatory movements were assessed across time, as previously described (Sobolewski et al., 2020).

4.4. Elevated plus maze

Mice underwent elevated plus maze testing as described previously (Merrill et al., 2022). Briefly, the elevated plus maze apparatus was made of black plastic and had two open arms (no sides; 34.9 × 6.07 cm), two closed arms (with sides; 34.9 × 6.07 × 19.13 cm), and a central platform (6.1 × 6.1 cm). Each mouse was placed in the center of the apparatus to start, and exploratory behavior was video recorded for 5 min. The amount of time spent in each area of the apparatus and the number of entries in the open arms, closed arms, and central hub was manually scored by an observer blind to experimental group.

4.5. Cortical tissue sample preparation

The week following behavioral testing (days 38–43), adult irradiated and control C57BL/6J, $P2Y12^{-/-}$, and CX3CR1−/− mice were euthanized and perfused intracardially with PBS. Hemispheres were separated and the cortex from one hemisphere was dissected and flash frozen. Cortical tissues were processed as described previously (Benraiss et al., 2022). Briefly, cortical tissues underwent homogenization by adding 1 mL of 5% SDS and 100 mM TEAB, followed by sonication (QSonica), and centrifugation to remove cellular debris. The supernatant was collected and protein concentration was assessed using BCA (Thermo Scientific). Samples were then diluted to 1 mg/mL in 5% SDS and 50 mM TEAB and protein (25 μg) was reduced with dithiothreitol to 2 mM, followed by incubation at 55 °C for 1 h. Iodoacetamide was added to 10 mM and allowed to alkylate the proteins for 30 min in the dark at room temperature. Phosphoric acid was added to 1.2%, followed by six volumes of 90% methanol and 100 mM TEAB. The resulting mixture was loaded into S-Trap micros (Protifi) and centrifuged at 4000×*g* for 1 min. The S-Traps containing trapped proteins were washed twice with 90% methanol and 100 mM TEAB. Then, 1 μg of trypsin in 20 μL of 100 mM TEAB was added to the S-Trap, followed by an additional 20 μL of TEAB to maintain sample moisture. Samples were incubated at 37 °C overnight. The following day, the S-Trap was centrifuged at 4000×*g* for 1 min to collect the digested peptides. Sequential additions of 0.1% TFA in acetonitrile and 0.1% TFA in 50% acetonitrile were introduced to the S-trap, centrifuged, and pooled. Finally, samples were frozen, dried in a Speed Vac (Labconco), and re-suspended in 0.1% trifluoroacetic acid before mass spectrometry analysis.

4.6. Quantitative liquid chromatography with tandem mass spectrometry (LC-MS/MS)

Peptides were introduced onto a self-assembled 30 cm C18 column packed with 1.8 μm beads (Sepax) via an Easy nLC-1200 HPLC system (Thermo Fisher), interfaced with a Fusion Lumos Tribrid mass spectrometer (Thermo Fisher). Solvent A comprised 0.1% formic acid in water, while solvent B consisted of 0.1% formic acid in 80% acetonitrile. Ions were ionized and transferred to the mass spectrometer through a Nanospray Flex source operating at 2 kV. The chromatographic gradient initiated at 3% B and held for 2 min, increased to 10% B over 6 min, then further ramped up to 38% B over 65 min. Subsequently, it surged to 90% B within 5 min and maintained for 3 min before reverting to initial conditions over 2 min, followed by re-equilibration for 7 min, culminating in a total run time of 90 min. The Fusion Lumos operated in data-independent acquisition mode. Full MS1 scans were conducted over a range of 395–1005 m/z, with a resolution of 60,000 at m/z 200, an AGC target of 4e5, and a maximum injection time of 50 ms. MS2 scans employed higher energy dissociation (HCD) with a staggered windowing scheme of 14 m/z with 7 m/z overlaps, and fragment ions were analyzed in the Orbitrap at a resolution of 15,000, with an AGC target of 4e5, and a maximum injection time of 23 ms.

The raw data underwent processing with DIA-NN version 1.8.1 (https://github.com/vdemichev/DIA-NN) (Demichev et al., 2020), employing library-free analysis mode. For library annotation, the mouse UniProt 'one protein sequence per gene' database (UP000000589_10090, downloaded 4/7/2021) was utilized with deep learning-based spectra and RT prediction activated. Precursor ion generation parameters included a maximum of 1 missed cleavage, 1 variable modification for Ox(M), peptide length range of 7–30, precursor charge range of 2–3, precursor m/z range of 400–1000, and fragment m/z range of 200–2000. Quantification settings were configured to 'Robust LC (high precision)' mode with RT-dependent cross-run normalization, MBR enabled, protein inferences set to 'Genes,' and 'Heuristic protein inference' disabled. MS1 and MS2 mass tolerances, along with scan window size, were determined automatically by the software. Subsequently, precursors were filtered based on library precursor q-value (1%), library protein group q-value (1%), and posterior error probability (50%). Protein quantification was conducted using the MaxLFQ algorithm via the DIA-NN R package (https://github.com/vdemichev/diann-rpackage), while the number of peptides quantified in each protein group was tallied using the DiannReportGenerator Package (https://github.com/kswovick/DIANN-Report-Generator) (Cox et al., 2014). Data was analyzed using Perseus before downstream analysis in R. Due to the nature of how protein abundances were determined, whereby proteins were only excluded if there were 2 or more missing values across groups, P2Y12−/−mice are assigned very low protein abundance values for P2Y12 expression, but P2Y12 was not removed from the list of detected proteins.

4.7. Principal component analysis

Principal component analysis was performed using the prcomp function in R studio (Version 2023.06.0+421). For PCA plots, samples are shown as individual data points and color coded by experimental conditions.

4.8. Weighted protein correlation network analysis

A weighted protein correlation network from the proteomic data was derived using the blockwiseModule WGCNA function in R studio (Version 2023.06.0+421). The following settings were used for WGCNA: soft threshold power beta = 8.5, merge cut height = 0.25, TOMType = signed. Module eigenproteins (ME) represent the largest/first principal component of all proteins within a module, as previously described (Zhao et al., 2020). Module membership (MM) was defined as

the correlation between protein expression and MEs. The top 20 intramodular hub proteins are those with the highest connectivity to other proteins, and were selected by p-value of MM. We identified the top 20 proteins that significantly correlated with each trait of interest by lowest p-value of Pearson correlation between traits and protein expression values (Benjamin Hochberg corrected p-value <0.05). The cor function in R was used to calculate the Pearson correlation between protein expression data and each trait. The corPvalueStudent function in R was used to calculate the Student asymptomatic p-value. P-values were corrected with the Benjamin Hochberg method. Protein accessions were mapped to gene names using the UniProt.ws package for data visualization.

4.9. Differential expression analysis

Differentially expressed proteins were identified using a student's t-test with Benjamin Hochberg corrected p-value <0.05 (with no Log2-FoldChange cutoff due to the small changes observed). Volcano plots showing differential expression were created using R studio ggplot2. The top 10 upregulated and downregulated proteins (DEPs) were those with the lowest p-value. The 234 sex-biased proteins were compared to the 1354 sex-biased proteins identified by Wingo et al. (2023) in human brain tissue to determine proteins identified by both studies. For Supplemental Fig. 7, Bulk RNA-seq data from postmortem normal-appearing non-tumor brain tissue from glioblastoma (NAGBM) patients that had received radiotherapy cancer treatment and region-matched brain tissue from unaffected control individuals were retrieved from GSE207821. Differential gene expression analysis was performed using the DESeq2 package in R studio (Version 2023.06.0+421). Genes with less than 10 gene counts were excluded from the analysis across all samples. Log2FoldChage was calculated with the DESeq function. Ensemble gene IDs and protein accessions were mapped to gene names using the UniProt.ws package. Linear regression analysis was performed between changes in protein expression between irradiation and control mice (IR vs. Control log2FoldChange) and changes in RNA expression between NAGBM and control patients (NAGBM vs. Control log2FoldChange) using the lm function. Significant correlations were determined by $p < 0.05$.

4.10. Gene ontology enrichment analysis

Proteins of interest were used to create the query list for gene ontology analysis of biological processes or cellular components using ShinyGO (Version 0.77, http://bioinformatics.sdstate.edu/go). The 6863 proteins detected across all samples was used as a background list for queries. Plots generated using ShinyGo were included in Figs. 2 and 3, depicting the top 10 biological processes, with FDR<0.05. Plots for Fig. 6 were generated with data from ShinyGo queries using R studio ggplot2 illustrating the top 5 biological processes and cellular components, with FDR<0.2.

4.11. Predominant cell type protein expression analysis

Proteins were assigned for the following cell types: astrocytes, endothelial cells, microglia, oligodendrocyte progenitor cells (OPCs), newly-formed oligodendrocytes, myelinating oligodendrocytes, neurons by using the online database (https://brainrnaseq.org/) made by Zhang et al. (2014). From the database, cell-type gene lists were curated for genes whose expression was predominant in the designated cell types. If gene expression was >2X the mean expression across cell types for a given cell type, that gene was assigned to the respective cell type. Genes were appropriately assigned to multiple cell types if expression was >2X the mean expression across cell types for more than one category, as described (Carroll et al., 2020). Genes of interest were queried against cell-type gene lists. Proteins that were not assigned a cell type were categorized as "non specific".

4.12. Statistical analysis

All statistical analysis was carried out using R Studio (Version 2023.06.0+421). For behavioral data, a linear model followed by ANOVA was used to examine the effects of sex, genotype, radiation, and their interactions (Sex X genotype, Sex X radiation, Genotype X radiation, Sex X genotype X radiation) on all parameters assessed. For time course data, repeated-measures linear mixed-effects model followed by ANOVA was used to examined effects of bin genotype, radiation, and their interactions (Bin X genotype, Bin X radiation, Genotype X radiation, Bin X genotype X radiation). Normality of the behavioral data were assessed using Q-Q residual plots and residual versus fitted plots. One Cx3CR1−/− mouse was excluded from the elevated plus maze analysis as it was determined to be an outlier upon inspection of the residual plot. Statistical significance was defined as $p < 0.05$ (bolded) or $p < 0.10$ (listed in Table 1 but not bolded, listed in Table 2 with ~). Post hoc Tukey's tests HSD were performed following ANOVA. Group means with the same letter, symbol, or shape are not significantly different, whereas group means with different letters, symbols, or shapes are significantly different. Significance was determined by a linear model followed by ANOVA and Tukey's post hoc testing ($p < 0.05$). For proteomic data, outliers were determined based on visual inspection of principal component analysis plots resulting in no samples being excluded from the analysis. Further statistical analysis for proteomic data is described for different analyses in the above sections.

CRediT authorship contribution statement

Alexandra O. Strohm: Conceptualization, Data curation, Formal analysis, Funding acquisition, Investigation, Methodology, Project administration, Supervision, Visualization, Writing – original draft. **Sadie Oldfield:** Formal analysis. **Eric Hernady:** Methodology. **Carl J. Johnston:** Methodology. **Brian Marples:** Conceptualization, Funding acquisition, Methodology, Resources, Writing – review & editing. **M. Kerry O'Banion:** Conceptualization, Funding acquisition, Resources, Writing – review & editing. **Ania K. Majewska:** Conceptualization, Funding acquisition, Resources, Supervision, Writing – review & editing.

Funding

This work was supported by NINDS R01 NS114480 (AKM), T32ES007026 (AOS), NASA 80NSSC21K0542 (MKO), a Joan Wright Goodman award from the University of Rochester (AOS), and an Ernest J. Del Monte Institute for Neuroscience Pilot Grant (MKO). Additionally, this work utilized the University of Rochester Wilmot Cancer Institute Imaging and Radiation Shared Resource and S10 NIH grant S100D021548 (BM).

Declaration of competing interest

The authors declare that they have no known competing financial interests or personal relationships that could have appeared to influence the work reported in this paper.

Acknowledgements

We would like to acknowledge the URMC mass Spectrometry Resource laboratory, in particular Kevin Welle and Kyle Swovick, for conducting mass spectrometry and proteomic quantification. We would also like to acknowledge the URMC behavioral sciences facility, especially Travis Covitz, for conducting the behavioral assays in this paper.

Appendix A. Supplementary data

Supplementary data to this article can be found online at https://doi.org/10.1016/j.bbih.2024.100911.

Data availability

Data will be made available on request.

References

Acharya, M.M., Green, K.N., Allen, B.D., Najafi, A.R., Syage, A., Minasyan, H., Le, M.T., Kawashita, T., Giedzinski, E., Parihar, V.K., West, B.L., Baulch, J.E., Limoli, C.L., 2016. Elimination of microglia improves cognitive function following cranial irradiation. Sci. Rep. 6, 31545.

Allen, B.D., Syage, A.R., Maroso, M., Baddour, A.A.D., Luong, V., Minasyan, H., Giedzinski, E., West, B.L., Soltesz, I., Limoli, C.L., Baulch, J.E., Acharya, M.M., 2020. Mitigation of helium irradiation-induced brain injury by microglia depletion. J. Neuroinflammation 17 (1), 159.

André, P., Delaney, S.M., LaRocca, T., Vincent, D., DeGuzman, F., Jurek, M., Koller, B., Phillips, D.R., Conley, P.B., 2003. P2Y12 regulates platelet adhesion/activation, thrombus growth, and thrombus stability in injured arteries. J. Clin. Invest. 112 (3), 398–406.

Arli, B., Irkec, C., Menevse, S., Yilmaz, A., Alp, E., 2013. Fractalkine gene receptor polymorphism in patients with multiple sclerosis. Int. J. Neurosci. 123 (1), 31–37.

Arnoux, I., Audinat, E., 2015. Fractalkine signaling and microglia functions in the developing brain. Neural Plast. 2015, 689404.

Badimon, A., Strasburger, H.J., Ayata, P., Chen, X., Nair, A., Ikegami, A., Hwang, P., Chan, A.T., Graves, S.M., Uweru, J.O., Ledderose, C., Kutlu, M.G., Wheeler, M.A., Kahan, A., Ishikawa, M., Wang, Y.C., Loh, Y.E., Jiang, J.X., Surmeier, D.J., Robson, S. C., Junger, W.G., Sebra, R., Calipari, E.S., Kenny, P.J., Eyo, U.B., Colonna, M., Quintana, F.J., Wake, H., Gradinaru, V., Schaefer, A., 2020. Negative feedback control of neuronal activity by microglia. Nature 586 (7829), 417–423.

Baldereschi, M., Di Carlo, A., Rocca, W.A., Vanni, P., Maggi, S., Perissinotto, E., Grigoletto, F., Amaducci, L., Inzitari, D., 2000. Parkinson's disease and parkinsonism in a longitudinal study: two-fold higher incidence in men. ILSA Working Group. Italian Longitudinal Study on Aging. Neurology 55 (9), 1358–1363.

Barko, K., Shelton, M., Xue, X., Afriyie-Agyemang, Y., Puig, S., Freyberg, Z., Tseng, G.C., Logan, R.W., Seney, M.L., 2022. Brain region- and sex-specific transcriptional profiles of microglia. Front. Psychiatr. 13, 945548.

Belarbi, K., Jopson, T., Arellano, C., Fike, J.R., Rosi, S., 2013. CCR2 deficiency prevents neuronal dysfunction and cognitive impairments induced by cranial irradiation. Cancer Res. 73 (3), 1201–1210.

Benraiss, A., Mariani, J.N., Tate, A., Madsen, P.M., Clark, K.M., Welle, K.A., Solly, R., Capellano, L., Bentley, K., Chandler-Militello, D., Goldman, S.A., 2022. A TCF7L2-responsive suppression of both homeostatic and compensatory remyelination in Huntington disease mice. Cell Rep. 40 (9), 111291.

Bhat, K., Medina, P., He, L., Zhang, L., Saki, M., Ioannidis, A., Nguyen, N.T., Sodhi, S.S., Sung, D., Magyar, C.E., Liau, L.M., Kornblum, H.I., Pajonk, F., 2020. 1-[(4-Nitrophenyl)sulfonyl]-4-phenylpiperazine treatment after brain irradiation preserves cognitive function in mice. Neuro Oncol. 22 (10), 1484–1494.

Boeddrich, A., Haenig, C., Neuendorf, N., Blanc, E., Ivanov, A., Kirchner, M., Schleumann, P., Bayraktaroglu, I., Richter, M., Molenda, C.M., Sporbert, A., Zenkner, M., Schnoegl, S., Suenkel, C., Schneider, L.S., Rybak-Wolf, A., Kochnowsky, B., Byrne, L.M., Wild, E.J., Nielsen, J.E., Dittmar, G., Peters, O., Beule, D., Wanker, E.E., 2023. A proteomics analysis of 5xFAD mouse brain regions reveals the lysosome-associated protein Arl8b as a candidate biomarker for Alzheimer's disease. Genome Med. 15 (1), 50.

Bollinger, J.L., Dadosky, D.T., Flurer, J.K., Rainer, I.L., Woodburn, S.C., Wohleb, E.S., 2023. Microglial P2Y12 mediates chronic stress-induced synapse loss in the prefrontal cortex and associated behavioral consequences. Neuropsychopharmacology 48 (9), 1347–1357.

Camacho-Hernandez, N.P., Pena-Ortega, F., 2023. Fractalkine/CX3CR1-Dependent modulation of synaptic and network plasticity in health and disease. Neural Plast. 2023, 4637073.

Cao, Q., Tan, C.C., Xu, W., Hu, H., Cao, X.P., Dong, Q., Tan, L., Yu, J.T., 2020. The prevalence of dementia: a systematic review and meta-analysis. J Alzheimers Dis 73 (3), 1157–1166.

Cardona, A.E., Pioro, E.P., Sasse, M.E., Kostenko, V., Cardona, S.M., Dijkstra, I.M., Huang, D., Kidd, G., Dombrowski, S., Dutta, R., Lee, J.C., Cook, D.N., Jung, S., Lira, S.A., Littman, D.R., Ransohoff, R.M., 2006. Control of microglial neurotoxicity by the fractalkine receptor. Nat. Neurosci. 9 (7), 917–924.

Carroll, J.A., Race, B., Williams, K., Striebel, J., Chesebro, B., 2020. RNA-seq and network analysis reveal unique glial gene expression signatures during prion infection. Mol. Brain 13 (1), 71.

Constanzo, J., Midavaine, E., Fouquet, J., Lepage, M., Descoteaux, M., Kirby, K., Tremblay, L., Masson-Cote, L., Geha, S., Longpre, J.M., Paquette, B., Sarret, P., 2020. Brain irradiation leads to persistent neuroinflammation and long-term neurocognitive dysfunction in a region-specific manner. Prog. Neuro-Psychopharmacol. Biol. Psychiatry 102, 109954.

Cornell, J., Salinas, S., Huang, H.Y., Zhou, M., 2022. Microglia regulation of synaptic plasticity and learning and memory. Neural Regen Res 17 (4), 705–716.

Corona, A.W., Huang, Y., O'Connor, J.C., Dantzer, R., Kelley, K.W., Popovich, P.G., Godbout, J.P., 2010. Fractalkine receptor (CX3CR1) deficiency sensitizes mice to the behavioral changes induced by lipopolysaccharide. J. Neuroinflammation 7, 93.

Cox, J., Hein, M.Y., Luber, C.A., Paron, I., Nagaraj, N., Mann, M., 2014. Accurate proteome-wide label-free quantification by delayed normalization and maximal peptide ratio extraction, termed MaxLFQ. Mol. Cell. Proteomics 13 (9), 2513–2526.

Cserep, C., Posfai, B., Lenart, N., Fekete, R., Laszlo, Z.I., Lele, Z., Orsolits, B., Molnar, G., Heindl, S., Schwarcz, A.D., Ujvari, K., Kornyei, Z., Toth, K., Szabadits, E., Sperlagh, B., Baranyi, M., Csiba, L., Hortobagyi, T., Magloczky, Z., Martinecz, B., Szabo, G., Erdelyi, F., Szipocs, R., Tamkun, M.M., Gesierich, B., Duering, M., Katona, I., Liesz, A., Tamas, G., Denes, A., 2020. Microglia monitor and protect neuronal function through specialized somatic purinergic junctions. Science 367 (6477), 528–537.

Cubello, J., Marvin, E., Conrad, K., Merrill, A.K., George, J.V., Welle, K., Jackson, B.P., Chalupa, D., Oberdorster, G., Sobolewski, M., Cory-Slechta, D.A., 2024. The contributions of neonatal inhalation of copper to air pollution-induced neurodevelopmental outcomes in mice. Neurotoxicology 100, 55–71.

Davalos, D., Grutzendler, J., Yang, G., Kim, J.V., Zuo, Y., Jung, S., Littman, D.R., Dustin, M.L., Gan, W.B., 2005. ATP mediates rapid microglial response to local brain injury in vivo. Nat. Neurosci. 8 (6), 752–758.

de Guzman, A.E., Ahmed, M., Perrier, S., Hammill, C., Li, Y.Q., Wong, C.S., Nieman, B.J., 2022. Protection from radiation-induced neuroanatomical deficits by CCL2-deficiency is dependent on sex. Int. J. Radiat. Oncol. Biol. 113, 390–400.

Demichev, V., Messner, C.B., Vernardis, S.I., Lilley, K.S., Ralser, M., 2020. DIA-NN: neural networks and interference correction enable deep proteome coverage in high throughput. Nat. Methods 17 (1), 41–44.

Distler, U., Schumann, S., Kesseler, H.G., Pielot, R., Smalla, K.H., Sielaff, M., Schmeisser, M.J., Tenzer, S., 2020. Proteomic analysis of brain region and sex-specific synaptic protein expression in the adult mouse brain. Cells 9 (2).

Duggan, M.R., Parikh, V., 2021. Microglia and modifiable life factors: potential contributions to cognitive resilience in aging. Behav. Brain Res. 405, 113207.

Fairley, L.H., Wong, J.H., Barron, A.M., 2021. Mitochondrial regulation of microglial immunometabolism in alzheimer's disease. Front. Immunol. 12, 624538.

Feng, X., Jopson, T.D., Paladini, M.S., Liu, S., West, B.L., Gupta, N., Rosi, S., 2016. Colony-stimulating factor 1 receptor blockade prevents fractionated whole-brain irradiation-induced memory deficits. J. Neuroinflammation 13 (1), 215.

Feng, X., Liu, S., Chen, D., Rosi, S., Gupta, N., 2018. Rescue of cognitive function following fractionated brain irradiation in a novel preclinical glioma model. Elife 7.

Fontana, A., Marin, B., Luna, J., Beghi, E., Logroscino, G., Boumediene, F., Preux, P.M., Couratier, P., Copetti, M., 2021. Time-trend evolution and determinants of sex ratio in Amyotrophic Lateral Sclerosis: a dose-response meta-analysis. J. Neurol. 268 (8), 2973–2984.

Gibson, E.M., Nagaraja, S., Ocampo, A., Tam, L.T., Wood, L.S., Pallegar, P.N., Greene, J. J., Geraghty, A.C., Goldstein, A.K., Ni, L., Woo, P.J., Barres, B.A., Liddelow, S., Vogel, H., Monje, M., 2019. Methotrexate chemotherapy induces persistent tri-glial dysregulation that underlies chemotherapy-related cognitive impairment. Cell 176 (1–2), 43–55 e13.

Goldblum, J.E., McFayden, T.C., Bristol, S., Putnam, O.C., Wylie, A., Harrop, C., 2023. Autism prevalence and the intersectionality of assigned sex at birth, race, and ethnicity on age of diagnosis. J. Autism Dev. 54, 3777–3791.

Greene-Schloesser, D., Robbins, M.E., 2012a. Radiation-induced cognitive impairment–from bench to bedside. Neuro Oncol. 14 (Suppl. 4), iv37–44. Suppl 4.

Greene-Schloesser, D., Robbins, M.E., Peiffer, A.M., Shaw, E.G., Wheeler, K.T., Chan, M. D., 2012b. Radiation-induced brain injury: a review. Front. Oncol. 2, 73.

Gu, N., Eyo, U.B., Murugan, M., Peng, J., Matta, S., Dong, H., Wu, L.J., 2016. Microglial P2Y12 receptors regulate microglial activation and surveillance during neuropathic pain. Brain Behav. Immun. 55, 82–92.

Guneykaya, D., Ivanov, A., Hernandez, D.P., Haage, V., Wojtas, B., Meyer, N., Maricos, M., Jordan, P., Buonfiglioli, A., Gielniewski, B., Ochocka, N., Comert, C., Friedrich, C., Artiles, L.S., Kaminska, B., Mertins, P., Beule, D., Kettenmann, H., Wolf, S.A., 2018. Transcriptional and translational differences of microglia from male and female brains. Cell Rep. 24 (10), 2773–2783 e6.

Gunner, G., Cheadle, L., Johnson, K.M., Ayata, P., Badimon, A., Mondo, E., Nagy, M.A., Liu, L., Bemiller, S.M., Kim, K.W., Lira, S.A., Lamb, B.T., Tapper, A.R., Ransohoff, R. M., Greenberg, M.E., Schaefer, A., Schafer, D.P., 2019. Sensory lesioning induces microglial synapse elimination via ADAM10 and fractalkine signaling. Nat. Neurosci. 22 (7), 1075–1088.

Han, W., Umekawa, T., Zhou, K., Zhang, X.M., Ohshima, M., Dominguez, C.A., Harris, R. A., Zhu, C., Blomgren, K., 2016. Cranial irradiation induces transient microglia accumulation, followed by long-lasting inflammation and loss of microglia. Oncotarget 7 (50), 82305–82323.

Hanamsagar, R., Alter, M.D., Block, C.S., Sullivan, H., Bolton, J.L., Bilbo, S.D., 2017. Generation of a microglial developmental index in mice and in humans reveals a sex difference in maturation and immune reactivity. Glia 65 (9), 1504–1520.

Harrison, J.K., Jiang, Y., Chen, S., Xia, Y., Maciejewski, D., McNamara, R.K., Streit, W.J., Salafranca, M.N., Adhikari, S., Thompson, D.A., Botti, P., Bacon, K.B., Feng, L., 1998. Role for neuronally derived fractalkine in mediating interactions between neurons and CX3CR1-expressing microglia. Proc. Natl. Acad. Sci. U.S.A. 95 (18), 10896–10901.

Haynes, S.E., Hollopeter, G., Yang, G., Kurpius, D., Dailey, M.E., Gan, W.B., Julius, D., 2006. The P2Y12 receptor regulates microglial activation by extracellular nucleotides. Nat. Neurosci. 9 (12), 1512–1519.

Hellwig, S., Brioschi, S., Dieni, S., Frings, L., Masuch, A., Blank, T., Biber, K., 2016. Altered microglia morphology and higher resilience to stress-induced depression-like behavior in CX3CR1-deficient mice. Brain Behav. Immun. 55, 126–137.

Hinkle, J.J., Olschowka, J.A., Love, T.M., Williams, J.P., O'Banion, M.K., 2019. Cranial irradiation mediated spine loss is sex-specific and complement receptor-3 dependent in male mice. Sci. Rep. 9 (1), 18899.

Hinkle, J.J., Olschowka, J.A., Williams, J.P., O'Banion, M.K., 2023. Pharmacologic manipulation of complement receptor 3 prevents dendritic spine loss and cognitive impairment after acute cranial radiation. Int. J. Radiat. Oncol. Biol. 119, 912–923.

Honda, S., Sasaki, Y., Ohsawa, K., Imai, Y., Nakamura, Y., Inoue, K., Kohsaka, S., 2001. Extracellular ATP or ADP induce chemotaxis of cultured microglia through Gi/o-coupled P2Y receptors. J. Neurosci. 21 (6), 1975–1982.
Ilic, I., Ilic, M., 2023. International patterns and trends in the brain cancer incidence and mortality: an observational study based on the global burden of disease. Heliyon 9 (7), e18222.
Ishizuka, K., Fujita, Y., Kawabata, T., Kimura, H., Iwayama, Y., Inada, T., Okahisa, Y., Egawa, J., Usami, M., Kushima, I., Uno, Y., Okada, T., Ikeda, M., Aleksic, B., Mori, D., Someya, T., Yoshikawa, T., Iwata, N., Nakamura, H., Yamashita, T., Ozaki, N., 2017. Rare genetic variants in CX3CR1 and their contribution to the increased risk of schizophrenia and autism spectrum disorders. Transl. Psychiatry 7 (8), e1184.
Jenrow, K.A., Brown, S.L., Lapanowski, K., Naei, H., Kolozsvary, A., Kim, J.H., 2013. Selective inhibition of microglia-mediated neuroinflammation mitigates radiation-induced cognitive impairment. Radiat. Res. 179 (5), 549–556.
Jockwitz, C., Wiersch, L., Stumme, J., Caspers, S., 2021. Cognitive profiles in older males and females. Sci. Rep. 11 (1), 6524.
Jung, S.Y., Choi, J.M., Rousseaux, M.W., Malovannaya, A., Kim, J.J., Kutzera, J., Wang, Y., Huang, Y., Zhu, W., Maity, S., Zoghbi, H.Y., Qin, J., 2017. An anatomically resolved mouse brain proteome reveals Parkinson disease-relevant pathways. Mol. Cell. Proteomics 16 (4), 581–593.
Kalm, M., Andreasson, U., Bjork-Eriksson, T., Zetterberg, H., Pekny, M., Blennow, K., Pekna, M., Blomgren, K., 2016. C3 deficiency ameliorates the negative effects of irradiation of the young brain on hippocampal development and learning. Oncotarget 7 (15), 19382–19394.
Kessler, R.C., Demler, O., Frank, R.G., Olfson, M., Pincus, H.A., Walters, E.E., Wang, P., Wells, K.B., Zaslavsky, A.M., 2005. Prevalence and treatment of mental disorders, 1990 to 2003. N. Engl. J. Med. 352 (24), 2515–2523.
Krukowski, K., Feng, X., Paladini, M.S., Chou, A., Sacramento, K., Grue, K., Riparip, L.K., Jones, T., Campbell-Beachler, M., Nelson, G., Rosi, S., 2018a. Temporary microglia-depletion after cosmic radiation modifies phagocytic activity and prevents cognitive deficits. Sci. Rep. 8 (1), 7857.
Krukowski, K., Grue, K., Frias, E.S., Pietrykowski, J., Jones, T., Nelson, G., Rosi, S., 2018b. Female mice are protected from space radiation-induced maladaptive responses. Brain Behav. Immun. 74, 106–120.
Lee, S.W., Haditsch, U., Cord, B.J., Guzman, R., Kim, S.J., Boettcher, C., Priller, J., Ormerod, B.K., Palmer, T.D., 2013. Absence of CCL2 is sufficient to restore hippocampal neurogenesis following cranial irradiation. Brain Behav. Immun. 30, 33–44.
Lee, H.-J., Kim, J.-S., Moon, C., Son, Y., 2022. Profiling of gene expression in the brain associated with anxiety-related behaviors in the chronic phase following cranial irradiation. Sci. Rep. 12 (1).
Leszczynski, D., 2014. Radiation proteomics: a brief overview. Proteomics 14 (4–5), 481–488.
Levine, D.A., Gross, A.L., Briceno, E.M., Tilton, N., Giordani, B.J., Sussman, J.B., Hayward, R.A., Burke, J.F., Hingtgen, S., Elkind, M.S.V., Manly, J.J., Gottesman, R. F., Gaskin, D.J., Sidney, S., Sacco, R.L., Tom, S.E., Wright, C.B., Yaffe, K., Galecki, A. T., 2021. Sex differences in cognitive decline among US adults. JAMA Netw. Open 4 (2), e210169.
Li, M.D., Burns, T.C., Kumar, S., Morgan, A.A., Sloan, S.A., Palmer, T.D., 2015. Aging-like changes in the transcriptome of irradiated microglia. Glia 63 (5), 754–767.
Lin, S.S., Tang, Y., Illes, P., Verkhratsky, A., 2020. The safeguarding microglia: central role for P2Y(12) receptors. Front. Pharmacol. 11, 627760.
Liu, B., Hinshaw, R.G., Le, K.X., Park, M.A., Wang, S., Belanger, A.P., Dubey, S., Frost, J. L., Shi, Q., Holton, P., Trojanczyk, L., Reiser, V., Jones, P.A., Trigg, W., Di Carli, M.F., Lorello, P., Caldarone, B.J., Williams, J.P., O'Banion, M.K., Lemere, C.A., 2019. Space-like (56)Fe irradiation manifests mild, early sex-specific behavioral and neuropathological changes in wildtype and Alzheimer's-like transgenic mice. Sci. Rep. 9 (1), 12118.
Lopez-Lopez, A., Gamez, J., Syriani, E., Morales, M., Salvado, M., Rodriguez, M.J., Mahy, N., Vidal-Taboada, J.M., 2014. CX3CR1 is a modifying gene of survival and progression in amyotrophic lateral sclerosis. PLoS One 9 (5), e96528.
Lowery, R.L., Tremblay, M.E., Hopkins, B.E., Majewska, A.K., 2017. The microglial fractalkine receptor is not required for activity-dependent plasticity in the mouse visual system. Glia 65 (11), 1744–1761.
Lowery, R.L., Mendes, M.S., Sanders, B.T., Murphy, A.J., Whitelaw, B.S., Lamantia, C.E., Majewska, A.K., 2021. Loss of P2Y12 has behavioral effects in the adult mouse. Int. J. Mol. Sci. 22 (4).
Maier, T., Guell, M., Serrano, L., 2009. Correlation of mRNA and protein in complex biological samples. FEBS Lett. 583 (24), 3966–3973.
Manolopoulos, P., Glenn, J.R., Fox, S.C., May, J.A., Dovlatova, N.L., Tang, S.W., Thomas, N.R., Ralevic, V., Heptinstall, S., 2008. Acyl derivatives of coenzyme A inhibit platelet function via antagonism at P2Y1 and P2Y12 receptors: a new finding that may influence the design of anti-thrombotic agents. Platelets 19 (2), 134–145.
Markarian, M., Krattli Jr., R.P., Baddour, J.D., Alikhani, L., Giedzinski, E., Usmani, M.T., Agrawal, A., Baulch, J.E., Tenner, A.J., Acharya, M.M., 2021. Glia-selective deletion of complement C1q prevents radiation-induced cognitive deficits and neuroinflammation. Cancer Res. 81 (7), 1732–1744.
Marras, C., Beck, J.C., Bower, J.H., Roberts, E., Ritz, B., Ross, G.W., Abbott, R.D., Savica, R., Van Den Eeden, S.K., Willis, A.W., Tanner, C.M., Parkinson's Foundation, P.G., 2018. Prevalence of Parkinson's disease across north America. NPJ Parkinsons Dis 4, 21.
McCarrey, A.C., An, Y., Kitner-Triolo, M.H., Ferrucci, L., Resnick, S.M., 2016. Sex differences in cognitive trajectories in clinically normal older adults. Psychol. Aging 31 (2), 166–175.
Mendez-Salcido, F.A., Torres-Flores, M.I., Ordaz, B., Pena-Ortega, F., 2022. Abnormal innate and learned behavior induced by neuron-microglia miscommunication is related to CA3 reconfiguration. Glia 70 (9), 1630–1651.
Merrill, A.K., Conrad, K., Marvin, E., Sobolewski, M., 2022. Effects of gestational low dose perfluorooctanoic acid on maternal and "anxiety-like" behavior in dams. Front Toxicol 4, 971970.
Milior, G., Lecours, C., Samson, L., Bisht, K., Poggini, S., Pagani, F., Deflorio, C., Lauro, C., Alboni, S., Limatola, C., Branchi, I., Tremblay, M.-E., Maggi, L., 2016. Fractalkine receptor deficiency impairs microglial and neuronal responsiveness to chronic stress. Brain Behav. Immun. 55, 114–125.
Moatti, D., Faure, S., Fumeron, F., Amara Mel, W., Seknadji, P., McDermott, D.H., Debre, P., Aumont, M.C., Murphy, P.M., de Prost, D., Combadiere, C., 2001. Polymorphism in the fractalkine receptor CX3CR1 as a genetic risk factor for coronary artery disease. Blood 97 (7), 1925–1928.
Monje, M.L., Mizumatsu, S., Fike, J.R., Palmer, T.D., 2002. Irradiation induces neural precursor-cell dysfunction. Nat. Med. 8 (9), 955–962.
Montay-Gruel, P., Acharya, M.M., Goncalves Jorge, P., Petit, B., Petridis, I.G., Fuchs, P., Leavitt, R., Petersson, K., Gondre, M., Ollivier, J., Moeckli, R., Bochud, F., Bailat, C., Bourhis, J., Germond, J.F., Limoli, C.L., Vozenin, M.C., 2021. Hypofractionated FLASH-RT as an effective treatment against glioblastoma that reduces neurocognitive side effects in mice. Clin. Cancer Res. 27 (3), 775–784.
Moravan, M.J., Olschowka, J.A., Williams, J.P., O'Banion, M.K., 2011. Cranial irradiation leads to acute and persistent neuroinflammation with delayed increases in T-cell infiltration and CD11c expression in C57BL/6 mouse brain. Radiat. Res. 176 (4), 459–473.
Moravan, M.J., Olschowka, J.A., Williams, J.P., O'Banion, M.K., 2016. Brain radiation injury leads to a dose- and time-dependent recruitment of peripheral myeloid cells that depends on CCR2 signaling. J. Neuroinflammation 13, 30.
Nemes-Baran, A.D., White, D.R., DeSilva, T.M., 2020. Fractalkine-dependent microglial pruning of viable oligodendrocyte progenitor cells regulates myelination. Cell Rep. 32 (7), 108047.
Nimmerjahn, A., Kirchhoff, F., Helmchen, F., 2005. Resting microglial cells are highly dynamic surveillants of brain parenchyma in vivo. Science 308 (5726), 1314–1318.
Njamnshi, A.K., Ahidjo, N., Ngarka, L., Nfor, L.N., Mengnjo, M.K., Njamnshi, W.Y., Basseguin Atchou, J.G., Tatah, G.Y., Mbaku, L.M., Dong, A.Z.F., Etet, P.F.S., 2020. Characterization of the cognitive and motor changes revealed by the elevated plus maze in an experimental rat model of radiation-induced brain injury. Adv. Biomed. Res. 9, 72.
Osman, A.M., Sun, Y., Burns, T.C., He, L., Kee, N., Oliva-Vilarnau, N., Alevyzaki, A., Zhou, K., Louhivuori, L., Uhlen, P., Hedlund, E., Betsholtz, C., Lauschke, V.M., Kele, J., Blomgren, K., 2020. Radiation triggers a dynamic sequence of transient microglial alterations in juvenile brain. Cell Rep. 31 (9), 107699.
Paolicelli, R.C., Bolasco, G., Pagani, F., Maggi, L., Scianni, M., Panzanelli, P., Giustetto, M., Ferreira, T.A., Guiducci, E., Dumas, L., Ragozzino, D., Gross, C.T., 2011. Synaptic pruning by microglia is necessary for normal brain development. Science 333 (6048), 1456–1458.
Parente, A., de Vries, E.F.J., van Waarde, A., Ioannou, M., van Luijk, P., Langendijk, J.A., Dierckx, R., Doorduin, J., 2020. The acute and early effects of whole-brain irradiation on glial activation, brain metabolism, and behavior: a positron emission tomography study. Mol. Imag. Biol. 22 (4), 1012–1020.
Parihar, V.K., Limoli, C.L., 2013. Cranial irradiation compromises neuronal architecture in the hippocampus. Proc. Natl. Acad. Sci. U.S.A. 110 (31), 12822–12827.
Parihar, V.K., Angulo, M.C., Allen, B.D., Syage, A., Usmani, M.T., Passerat de la Chapelle, E., Amin, A.N., Flores, L., Lin, X., Giedzinski, E., Limoli, C.L., 2020. Sex-specific cognitive deficits following space radiation exposure. Front. Behav. Neurosci. 14, 535885.
Peng, J., Liu, Y., Umpierre, A.D., Xie, M., Tian, D.S., Richardson, J.R., Wu, L.J., 2019. Microglial P2Y12 receptor regulates ventral hippocampal CA1 neuronal excitability and innate fear in mice. Mol. Brain 12 (1), 71.
Raber, J., Rola, R., LeFevour, A., Morhardt, D., Curley, J., Mizumatsu, S., VandenBerg, S. R., Fike, J.R., 2004. Radiation-induced cognitive impairments are associated with changes in indicators of hippocampal neurogenesis. Radiat. Res. 162 (1), 39–47.
Rimmerman, N., Schottlender, N., Reshef, R., Dan-Goor, N., Yirmiya, R., 2017. The hippocampal transcriptomic signature of stress resilience in mice with microglial fractalkine receptor (CX3CR1) deficiency. Brain Behav. Immun. 61, 184–196.
Rogers, J.T., Morganti, J.M., Bachstetter, A.D., Hudson, C.E., Peters, M.M., Grimmig, B. A., Weeber, E.J., Bickford, P.C., Gemma, C., 2011. CX3CR1 deficiency leads to impairment of hippocampal cognitive function and synaptic plasticity. J. Neurosci. 31 (45), 16241–16250.
Roughton, K., Kalm, M., Blomgren, K., 2012. Sex-dependent differences in behavior and hippocampal neurogenesis after irradiation to the young mouse brain. Eur. J. Neurosci. 36 (6), 2763–2772.
Schwarz, J.M., Sholar, P.W., Bilbo, S.D., 2012. Sex differences in microglial colonization of the developing rat brain. J. Neurochem. 120 (6), 948–963.
Sharma, K., Schmitt, S., Bergner, C.G., Tyanova, S., Kannaiyan, N., Manrique-Hoyos, N., Kongi, K., Cantuti, L., Hanisch, U.K., Philips, M.A., Rossner, M.J., Mann, M., Simons, M., 2015. Cell type- and brain region-resolved mouse brain proteome. Nat. Neurosci. 18 (12), 1819–1831.
Shukla, S., Shankavaram, U.T., Nguyen, P., Stanley, B.A., Smart, D.K., 2015. Radiation-induced alteration of the brain proteome: understanding the role of the sirtuin 2 deacetylase in a murine model. J. Proteome Res. 14 (10), 4104–4117.
Sipe, G.O., Lowery, R.L., Tremblay, M.E., Kelly, E.A., Lamantia, C.E., Majewska, A.K., 2016. Microglial P2Y12 is necessary for synaptic plasticity in mouse visual cortex. Nat. Commun. 7, 10905.
Sobolewski, M., Abston, K., Conrad, K., Marvin, E., Harvey, K., Susiarjo, M., Cory-Slechta, D.A., 2020. Lineage- and sex-dependent behavioral and biochemical

transgenerational consequences of developmental exposure to lead, prenatal stress, and combined lead and prenatal stress in mice. Environ. Health Perspect. 128 (2), 27001.
Sokolowski, J.D., Chabanon-Hicks, C.N., Han, C.Z., Heffron, D.S., Mandell, J.W., 2014. Fractalkine is a "find-me" signal released by neurons undergoing ethanol-induced apoptosis. Front. Cell. Neurosci. 8, 360.
Stenken, J.A., Poschenrieder, A.J., 2015. Bioanalytical chemistry of cytokines–a review. Anal. Chim. Acta 853, 95–115.
Strohm, A.O., Johnston, C., Hernady, E., Marples, B., O'Banion, M.K., Majewska, A.K., 2024. Cranial irradiation disrupts homeostatic microglial dynamic behavior. J. Neuroinflammation 21 (1).
Thion, M.S., Low, D., Silvin, A., Chen, J., Grisel, P., Schulte-Schrepping, J., Blecher, R., Ulas, T., Squarzoni, P., Hoeffel, G., Coulpier, F., Siopi, E., David, F.S., Scholz, C., Shihui, F., Lum, J., Amoyo, A.A., Larbi, A., Poidinger, M., Buttgereit, A., Lledo, P.M., Greter, M., Chan, J.K.Y., Amit, I., Beyer, M., Schultze, J.L., Schlitzer, A., Pettersson, S., Ginhoux, F., Garel, S., 2018. Microbiome influences prenatal and adult microglia in a sex-specific manner. Cell 172 (3), 500–516 e16.
Tome, W.A., Gokhan, S., Brodin, N.P., Gulinello, M.E., Heard, J., Mehler, M.F., Guha, C., 2015. A mouse model replicating hippocampal sparing cranial irradiation in humans: a tool for identifying new strategies to limit neurocognitive decline. Sci. Rep. 5, 14384.
Tuo, J., Smith, B.C., Bojanowski, C.M., Meleth, A.D., Gery, I., Csaky, K.G., Chew, E.Y., Chan, C.C., 2004. The involvement of sequence variation and expression of CX3CR1 in the pathogenesis of age-related macular degeneration. Faseb. J. 18 (11), 1297–1299.
Uweru, O.J., Okojie, A.K., Trivedi, A., Benderoth, J., Thomas, L.S., Davidson, G., Cox, K., Eyo, U.B., 2024. A P2RY12 deficiency results in sex-specific cellular perturbations and sexually dimorphic behavioral anomalies. J. Neuroinflammation 21 (1), 95.
Vasek, M.J., Mueller, S.M., Fass, S.B., Deajon-Jackson, J.D., Liu, Y., Crosby, H.W., Koester, S.K., Yi, J., Li, Q., Dougherty, J.D., 2023. Local translation in microglial processes is required for efficient phagocytosis. Nat. Neurosci. 26 (7), 1185–1195.
Villa, A., Gelosa, P., Castiglioni, L., Cimino, M., Rizzi, N., Pepe, G., Lolli, F., Marcello, E., Sironi, L., Vegeto, E., Maggi, A., 2018. Sex-specific features of microglia from adult mice. Cell Rep. 23 (12), 3501–3511.
Vogel, C., Marcotte, E.M., 2012. Insights into the regulation of protein abundance from proteomic and transcriptomic analyses. Nat. Rev. Genet. 13 (4), 227–232.
Walton, C., King, R., Rechtman, L., Kaye, W., Leray, E., Marrie, R.A., Robertson, N., La Rocca, N., Uitdehaag, B., van der Mei, I., Wallin, M., Helme, A., Angood Napier, C., Rijke, N., Baneke, P., 2020. Rising prevalence of multiple sclerosis worldwide: insights from the Atlas of MS, third edition. Mult. Scler. 26 (14), 1816–1821.
Wang, J., Pan, H., Lin, Z., Xiong, C., Wei, C., Li, H., Tong, F., Dong, X., 2021. Neuroprotective effect of fractalkine on radiation-induced brain injury through promoting the M2 polarization of microglia. Mol. Neurobiol. 58 (3), 1074–1087.
Wang, Q., Shi, N.R., Lv, P., Liu, J., Zhang, J.Z., Deng, B.L., Zuo, Y.Q., Yang, J., Wang, X., Chen, X., Hu, X.M., Liu, T.T., Liu, J., 2023. P2Y12 receptor gene polymorphisms are associated with epilepsy. Purinergic Signal. 19 (1), 155–162.
Webster, C.M., Hokari, M., McManus, A., Tang, X.N., Ma, H., Kacimi, R., Yenari, M.A., 2013. Microglial P2Y12 deficiency/inhibition protects against brain ischemia. PLoS One 8 (8), e70927.
Weickert, C.S., Elashoff, M., Richards, A.B., Sinclair, D., Bahn, S., Paabo, S., Khaitovich, P., Webster, M.J., 2009. Transcriptome analysis of male–female differences in prefrontal cortical development. Mol. Psychiatr. 14 (6), 558–561.
Weis, S.N., Souza, J.M.F., Hoppe, J.B., Firmino, M., Auer, M., Ataii, N.N., da Silva, L.A., Gaelzer, M.M., Klein, C.P., Mol, A.R., de Lima, C.M.R., Souza, D.O., Salbego, C.G., Ricart, C.A.O., Fontes, W., de Sousa, M.V., 2021. In-depth quantitative proteomic characterization of organotypic hippocampal slice culture reveals sex-specific differences in biochemical pathways. Sci. Rep. 11 (1), 2560.
Whitelaw, B.S., Tanny, S., Johnston, C.J., Majewska, A.K., O'Banion, M.K., Marples, B., 2021. In vivo imaging of the microglial landscape after whole brain radiation therapy. Int. J. Radiat. Oncol. Biol. 111, 1066–1071.
Whitelaw, B.S., Stoessel, M.B., Majewska, A.K., 2022. Movers and shakers: microglial dynamics and modulation of neural networks. Glia 71, 1575–1591.
Wingo, A.P., Liu, Y., Gerasimov, E.S., Vattathil, S.M., Liu, J., Cutler, D.J., Epstein, M.P., Blokland, G.A.M., Thambisetty, M., Troncoso, J.C., Duong, D.M., Bennett, D.A., Levey, A.I., Seyfried, N.T., Wingo, T.S., 2023. Sex differences in brain protein expression and disease. Nat. Med. 29 (9), 2224–2232.
Winter, A.N., Subbarayan, M.S., Grimmig, B., Weesner, J.A., Moss, L., Peters, M., Weeber, E., Nash, K., Bickford, P.C., 2020. Two forms of CX3CL1 display differential activity and rescue cognitive deficits in CX3CL1 knockout mice. J. Neuroinflammation 17 (1), 157.
Xu, J., Watkins, R., Arnold, A.P., 2006. Sexually dimorphic expression of the X-linked gene Eif2s3x mRNA but not protein in mouse brain. Gene Expr. Patterns 6 (2), 146–155.
Xu, P., Xu, Y., Hu, B., Wang, J., Pan, R., Murugan, M., Wu, L.J., Tang, Y., 2015. Extracellular ATP enhances radiation-induced brain injury through microglial activation and paracrine signaling via P2X7 receptor. Brain Behav. Immun. 50, 87–100.
Xu, Y., Hu, W., Liu, Y., Xu, P., Li, Z., Wu, R., Shi, X., Tang, Y., 2016. P2Y6 receptor-mediated microglial phagocytosis in radiation-induced brain injury. Mol. Neurobiol. 53 (6), 3552–3564.
Yu, T., Zhang, X., Shi, H., Tian, J., Sun, L., Hu, X., Cui, W., Du, D., 2019. P2Y12 regulates microglia activation and excitatory synaptic transmission in spinal lamina II neurons during neuropathic pain in rodents. Cell Death Dis. 10 (3), 165.
Yu, F., Wang, Y., Stetler, A.R., Leak, R.K., Hu, X., Chen, J., 2022. Phagocytic microglia and macrophages in brain injury and repair. CNS Neurosci. Ther. 28 (9), 1279–1293.
Zhan, Y., Paolicelli, R.C., Sforazzini, F., Weinhard, L., Bolasco, G., Pagani, F., Vyssotski, A.L., Bifone, A., Gozzi, A., Ragozzino, D., Gross, C.T., 2014. Deficient neuron-microglia signaling results in impaired functional brain connectivity and social behavior. Nat. Neurosci. 17 (3), 400–406.
Zhang, Y., Chen, K., Sloan, S.A., Bennett, M.L., Scholze, A.R., O'Keeffe, S., Phatnani, H.P., Guarnieri, P., Caneda, C., Ruderisch, N., Deng, S., Liddelow, S.A., Zhang, C., Daneman, R., Maniatis, T., Barres, B.A., Wu, J.Q., 2014. An RNA-sequencing transcriptome and splicing database of glia, neurons, and vascular cells of the cerebral cortex. J. Neurosci. 34 (36), 11929–11947.
Zhang, D., Zhou, W., Lam, T.T., Weng, C., Bronk, L., Ma, D., Wang, Q., Duman, J.G., Dougherty, P.M., Grosshans, D.R., 2018. Radiation induces age-dependent deficits in cortical synaptic plasticity. Neuro Oncol. 20 (9), 1207–1214.
Zhang, D., Zhou, W., Lam, T.T., Li, Y., Duman, J.G., Dougherty, P.M., Grosshans, D.R., 2020. Cranial irradiation induces axon initial segment dysfunction and neuronal injury in the prefrontal cortex and impairs hippocampal coupling. Neurooncol Adv 2 (1), vdaa058.
Zhao, N., Ren, Y., Yamazaki, Y., Qiao, W., Li, F., Felton, L.M., Mahmoudiandehkordi, S., Kueider-Paisley, A., Sonoustoun, B., Arnold, M., Shue, F., Zheng, J., Attrebi, O.N., Martens, Y.A., Li, Z., Bastea, L., Meneses, A.D., Chen, K., Thompson, J.W., St John-Williams, L., Tachibana, M., Aikawa, T., Oue, H., Job, L., Yamazaki, A., Liu, C.C., Storz, P., Asmann, Y.W., Ertekin-Taner, N., Kanekiyo, T., Kaddurah-Daouk, R., Bu, G., 2020. Alzheimer's risk factors age, APOE genotype, and sex drive distinct molecular pathways. Neuron 106 (5), 727–742 e6.
Zheng, F., Zhou, Q., Cao, Y., Shi, H., Wu, H., Zhang, B., Huang, F., Wu, X., 2019. P2Y(12) deficiency in mouse impairs noradrenergic system in brain, and alters anxiety-like neurobehavior and memory. Gene Brain Behav. 18 (2), e12458.